AUTOPHAGY
2022, VOL. 18, NO. 12, 2799–2816
https://doi.org/10.1080/15548627.2022.2047481

Taylor & Francis
Taylor & Francis Group

RESEARCH PAPER

KAT7-mediated CANX (calnexin) crotonylation regulates leucine-stimulated MTORC1 activity

Guokai Yan[a,b,c,†], Xiuzhi Li[a,b,c,†], Zilong Zheng[a,b,c], Weihua Gao[a,b,c], Changqing Chen[a,b,c], Xinkai Wang[a,b,c], Zhongyi Cheng[d], Jie Yu[a,e], Geng Zou[b,f], Muhammad Zahid Farooq[a,b,c], Xiaoyan Zhu[a,b,c], Weiyun Zhu[g], Qing Zhong[h], and Xianghua Yan[a,b,c]

[a]State Key Laboratory of Agricultural Microbiology, College of Animal Sciences and Technology, Huazhong Agricultural University, Wuhan, Hubei, China; [b]The Cooperative Innovation Center for Sustainable Pig Production, Wuhan, Hubei, China; [c]Hubei Provincial Engineering Laboratory for Pig Precision Feeding and Feed Safety Technology, Wuhan, Hubei, China; [d]Jingjie Ptm BioLab (Hangzhou), Co. Ltd, Hangzhou, Zhejiang, China; [e]Institute of Animal Husbandry and Veterinary, Wuhan Academy of Agricultural Science, Wuhan, Hubei, China; [f]College of Veterinary Medicine, Huazhong Agricultural University, Wuhan, Hubei, China; [g]College of Animal Science and Technology, Nanjing Agricultural University, Nanjing, Jiangsu, China; [h]Department of Pathophysiology, Key Laboratory of Cell Differentiation and Apoptosis of National Ministry of Education, Shanghai Jiao Tong University School of Medicine, Shanghai, China

ABSTRACT

Amino acids play crucial roles in the MTOR (mechanistic target of rapamycin kinase) complex 1 (MTORC1) pathway. However, the underlying mechanisms are not fully understood. Here, we establish a cell-free system to mimic the activation of MTORC1, by which we identify CANX (calnexin) as an essential regulator for leucine-stimulated MTORC1 pathway. CANX translocates to lysosomes after leucine deprivation, and its loss of function renders either the MTORC1 activity or the lysosomal translocation of MTOR insensitive to leucine deprivation. We further find that CANX binds to LAMP2 (lysosomal associated membrane protein 2), and LAMP2 is required for leucine deprivation-induced CANX interaction with the Ragulator to inhibit Ragulator activity toward RRAG GTPases. Moreover, leucine deprivation promotes the lysine (K) 525 crotonylation of CANX, which is another essential condition for the lysosomal translocation of CANX. Finally, we find that KAT7 (lysine acetyltransferase 7) mediates the K525 crotonylation of CANX. Loss of KAT7 renders the MTORC1 insensitivity to leucine deprivation. Our findings provide new insights for the regulatory mechanism of the leucine-stimulated MTORC1 pathway.

ARTICLE HISTORY
Received 17 April 2020
Revised 24 February 2021
Accepted 26 February 2021

KEYWORDS
CANX; KAT7; LAMP2; leucine; lysine crotonylation; MTORC1; ragulator

Introduction

The homeostasis of a cell needs the degradation and subsequently new synthesis of proteins. One of the most important cellular signaling pathways that fine-tunes protein homeostasis is mediated by MTOR (mechanistic target of rapamycin kinase), an atypical serine/threonine kinase involved in various biological processes mainly by phosphorylating key mediators in different pathways [1,2]. When complexed with AKT1S1/PRAS40 (AKT substrate 1), MLST8/GβL (MTOR associated protein, LST8 homolog), DEPTOR (DEP domain containing MTOR interacting protein), and RPTOR/Raptor (regulatory associated protein of MTOR complex 1) into the MTOR complex 1 (MTORC1) [3], the MTOR protein integrates signals by coordinating nutrients (such as amino acids, especially leucine) input with biosynthetic output, including promoting mRNA translation to facilitate synthesis of proteins [4,5]. The MTORC1 promotes protein synthesis largely through independently phosphorylating two key protein synthesis-controlling substrates, RPS6KB1/p70S6 kinase 1 (ribosomal protein S6 kinase B1) and EIF4EBP1 (eukaryotic translation initiation factor 4E binding protein 1) [6,7]. RPS6KB1, as a kinase, phosphorylates and activates several proteins that promote mRNA translation, including EIF4B (eukaryotic translation initiation factor 4B) [7,8], while EIF4EBP1 inhibits translation by preventing the assembly of the eukaryotic translation initiation factor 4 F complex, which controls the elongation of translation process [7]. For the activation of MTORC1 by amino acids, MTORC1 needs to translocate to the lysosome surface, where MTORC1 directly or indirectly binds to several regulatory proteins for its activation [9]. Once activated on the lysosome surface, MTOR functions as kinase to phosphorylate its substrates. All the core components of MTORC1 are crucial for MTOR function. Among them, RPTOR promotes the recruitment of substrates to the MTORC1 for their phosphorylation, and is necessary for the lysosomal localization of MTORC1 by acting as the direct binding site for the RRAG GTPase obligate heterodimers (RRAGA-RRAGB with RRAGC-RRAGD) [10], which bind to the LAMTOR (late endosomal/lysosomal adaptor, MAPK and MTOR activator) complex (also known as the Ragulator complex; composed of LAMTOR1 to LAMTOR5) that are located on the lysosome surface [9,11]. In addition,

CONTACT Xianghua Yan xhyan@mail.hzau.edu.cn State Key Laboratory of Agricultural Microbiology, College of Animal Sciences and Technology, Huazhong Agricultural University; The Cooperative Innovation Center for Sustainable Pig Production; Hubei Provincial Engineering Laboratory for Pig Precision Feeding and Feed Safety Technology, Wuhan, Hubei 430070, China
[†]These authors contributed equally to this work.
Supplemental data for this article can be accessed here.

a number of crucial regulatory proteins or protein complexes, such as GATOR1 (composed of DEPDC5 [DEP domain containing 5, GATOR1 subcomplex subunit], NPRL2 [NPR2 like, GATOR1 complex subunit], and NPRL3), GATOR2 (composed of SEC13 [SEC13 homolog, nuclear pore and COPII coat complex component], SEH1L [SEH1 like nucleoporin], MIOS [meiosis regulator for oocyte development], WDR59 [WD repeat domain 59], and WDR24), SLC7A5 (solute carrier family 7 member 5), and KICSTOR (composed of KPTN [kaptin, actin binding protein], ITFG2 [integrin alpha FG-GAP repeat containing protein 2], SZT2 [SZT2 subunit of KICSTOR complex], and KICS2 [KICSTOR subunit 2]), and TSC2 (TSC complex subunit 2), have been continuously found to have the requirement to be located onto the lysosome surface for the activation of MTORC1 [6].

Post-translational modifications (PTMs) play fundamental roles in almost all physiological and pathological processes. The MTORC1 pathway is regulated by several mechanisms including interacting proteins, subcellular localization, and/or PTMs. Phosphorylation and acetylation events have been shown to be involved in the MTORC1 regulation. Phosphorylation modifications at numerous sites of MTOR, such as Ser2159, Thr2164, Ser2448, and Ser2481, have crucial regulatory roles in MTORC1 kinase activity [12–14]. Meanwhile, RPTOR phosphorylation modifications mediated by multiple upstream kinases, such as AMP-activated protein kinase (AMPK) [15], DAPK2 (death associated protein kinase 2) [16], and ULK1 (unc-51 like autophagy activating kinase 1) [17], regulate MTORC1 activity via different mechanisms. In addition, the acetyltransferase EP300 (E1A binding protein p300)-mediated Lys1097 acetylation of RPTOR induced by leucine-derived metabolite acetyl-CoA has been shown to regulate the MTORC1 activity in certain cell types [18]. The acetylation of TSC2 may be also associated with MTORC1 regulation [19]. Due to dramatic development of integrated and mass spectrometry-based proteomic technologies, many new types of PTMs, such as lysine propionylation, butyrylation, and crotonylation, have been continuously identified over the past years [20]. Many newly identified PTMs were identified as acylation modifications in lysine residues of histones, which connects the acylation with epigenetic regulation of gene expression. However, less is known about the functions of these PTMs beyond regulating gene expression via modifying the histones.

In vitro reconstitution of biological processes, a fundamental complementation for the living cell investigation, has been applied as a crucial strategy to refine molecular models of biological processes. This strategy allows to mimic and manipulate biological processes directly by removing physical barriers [21]. In addition, *in vitro* reconstitution usually involves components in certain cellular space, thus well suitable for investigating the biological organization arose in specific compartment [22]. For instance, by *in vitro* reconstitution of biological process in cytosol, undesirable genetic regulations will be eliminated due to the removal of genomic DNA [23]. Moreover, by simplifying the complicated environment of cells, researchers may get new insights, such as identifying new members, for certain biological pathways. Previously, we have *in vitro* reconstituted the leucine-mediated macroautophagy/autophagy process, and found that the MTORC1-ATG14 (autophagy related 14) pathway played a central role in this process, which was also validated by *in vivo* assays [24]. Based on the well-established strategy, in the current study, we established another cell-free system, which can mimic the activation of MTORC1 by monitoring the lysosomal translocation of a readout protein RPTOR. Moreover, based on the established system, we identified an essential regulator CANX (calnexin) for leucine-stimulated protein synthetic MTORC1 pathway. Our study uncovered a previously unknown mechanism for regulation of MTORC1 activity.

Results

In vitro *reconstitution of leucine-stimulated MTORC1 activation*

Leucine stimulates MTORC1 activity by promoting MTORC1 translocation to the lysosome (Figure 1A; Fig. S1A). RPTOR/Raptor is a specific component of MTORC1, and MTORC1 binds to the RRAG GTPases via RPTOR in nutrient replete condition (Figure 1A). In addition, a previous study has used MYC-RPTOR or highly purified FLAG-RPTOR as indicators in *in vitro* cell-free systems that recapitulate the amino acid-induced translocation of MTORC1 to the lysosomal RRAG GTPases [25]. Based on this practice, we first aimed to conduct *in vitro* assays using RPTOR-lysosome association as readout to mimic the leucine-stimulated activation of MTORC1. For this purpose, we first purified the recombinant full-length hemagglutinin (HA)-RPTOR protein from HEK293T (human embryonic kidney-293 T) cells (Figure 1B; **Fig. S1B**). To prepare the lysosome or cytosol fractions, we cultured HEK293T cells with fresh complete or amino acid-free media, and fractionated the crude lysosome fraction (CLF) as CLF(+) and CLF(-), and the cytosol fraction as S100(+) and S100(-), respectively. The CLF(+), CLF(-), S100(+) and S100(-) were confirmed purified with other markers of cellular compartments (Figure 1C). In addition, the key regulators for MTORC1 lysosomal translocation, including RRAGA, RRAGC, and LAMTOR1, were all enriched in both the CLF(+) and CLF(-) (Figure 1D). These results confirmed that the fractions CLF and S100 could serve as lysosome and cytosol fractions for the subsequent *in vitro* assays.

Next we tested whether cytosolic factors can affect RPTOR-lysosome association in *in vitro* cell-free systems. We incubated S100(+) or S100(-) with recombinant HA-RPTOR, CLF(+) or CLF(-), with or without leucine supplementation. After centrifugation, the lysosome-containing pellet fractions were immunoblotted with antibodies against HA and lysosome marker LAMP2 (lysosomal associated membrane protein 2). The incubation of HA-RPTOR, CLF(+), and S100(-) was not bioactive (**Fig. S1C**). However, CLF(-) blocked the association of RPTOR and lysosomes (Figure 1E,

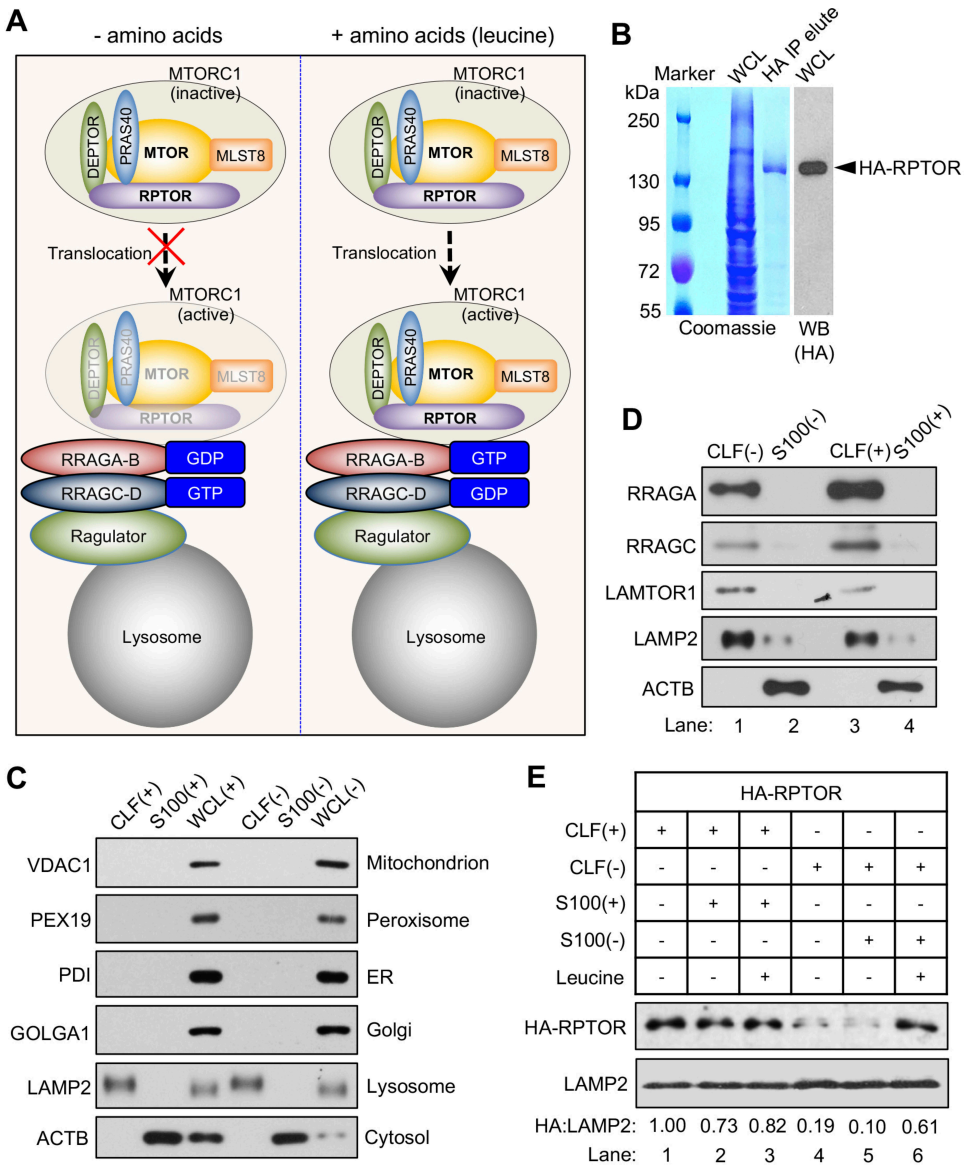

Figure 1. *In vitro* reconstitution of leucine-stimulated MTORC1 activity. (A) A schematic of the leucine-stimulated MTORC1 activation. (B) Purity test of recombinant HA-RPTOR purified from HEK293T cells. (C) Purity test for the purified lysosomal and cytosol fractions. HEK293T cells were cultured with fresh complete or amino acid-free media for 1 h to respectively fractionate the lysosome fraction as CLF(+) (left) and CLF(-) (right), while the supernatant from centrifugation at 100,000 x g (S100) were considered as cytosol fractions. ER, endoplasmic reticulum. (D) The immunoblotting test of the key MTORC1 regulators including RRAGA, RRAGC, LAMTOR1 for the CLF and S100 fractions. (E) The establishment of cell-free system for the leucine-stimulated MTORC1 activity. S100(+) or S100(-) was incubated with recombinant HA-RPTOR, CLF(+) or CLF(-), with or without leucine at 37°C for 30 min. After centrifugation, the pellet fractions were immunoblotted with antibodies against HA and LAMP2.

lane 4 compared with lane 1), suggesting amino acids-starved lysosomes inhibited the translocation of MTORC1 to lysosomes. In addition, the inhibitory activity by CLF(-) can not be attenuated by amino acids-starved cytosol fraction S100(-) (Figure 1E, lane 5 compared with lanes 2 and 4). Interestingly, leucine supplementation significantly attenuated the inhibition of association of RPTOR and lysosomes by CLF(-) and S100(-) by promoting the binding of RPTOR to the RRAG GTPases (Figure 1E, lane 6 compared with lane 5; **Fig. S1D**). Together, these results demonstrate that the reconstituted cell-free system containing CLF(-), S100(-), and HA-RPTOR were bioactive *in vitro*, and the system can be regulated by leucine.

Identification of CANX as an essential regulator for leucine-stimulated MTORC1 pathway

In order to identify new players in the leucine-stimulated MTORC1 pathway, we incubated the S100(-), CLF(-), HA-RPTOR, and with (group +Leu) or without (group Control) leucine supplementation to get a final volume of 100 μL for each sample for the MTORC1 system. After gently and sufficiently mixed, 5 samples were pooled into one sample for either Control or +Leu to reduce the individual error [26], and the pooled samples were centrifuged to collect the supernatant and pellet fractions. The supernatant and pellet fractions of Control and

+Leu were labeled with different iTRAQ (isobaric tags for relative and absolute quantification) reagents, mixed, and analyzed by LC-MS/MS (liquid chromatography-tandem mass spectrometry) (**Fig. S2A**). By this comparative proteomics-based strategy, a total of 41 proteins had differential abundances between Control supernatant fraction (S1) and +Leu supernatant fraction (S2), including 30 proteins that had higher abundances while 11 proteins that had lower abundances in S2 compared with S1 (Figure 2A; **Table S1**). In addition, 534 proteins had differential abundances between Control pellet fraction (P1) and +Leu pellet fraction (P2), including 279 proteins that had higher abundances while 255 proteins that had lower abundances in P2 compared with P1 (Figure 2A; **Table S2**). Notably, 13 proteins, including the leucine sensor SESN2 (sestrin 2), had higher abundances in S2 compared with S1, while had lower abundances in P2 compared with P1 (Figure 2A; **Table S3**). The differentially abundant proteins from the system were mainly localized to cytosol (**Fig. S2B**). Among all the differentially abundant proteins, CANX (calnexin) was less abundant in the lysosome pellet fractions while more abundant in the cytosol S100 fractions after leucine supplementation from our comparative proteomic analysis; meanwhile, previous study has implicated that CANX is a regulator for the autophagy pathway [27], which is one of the main downstream biological processes controlled by MTORC1 [6]. These raise a possibility that CANX is a potential MTORC1 regulator. To test this hypothesis, we first tested the abundance of CANX in the fractions of S1, S2, P1, and P2 from the cell-free system by immunoblotting assays (Figure 2B), and confirmed that CANX had higher abundance in S2 compared with S1, while had lower abundance in P2 compared with P1 (Figure 2C), which was in line with the proteomics data. In addition, using another well-established immunoprecipitation (IP)-

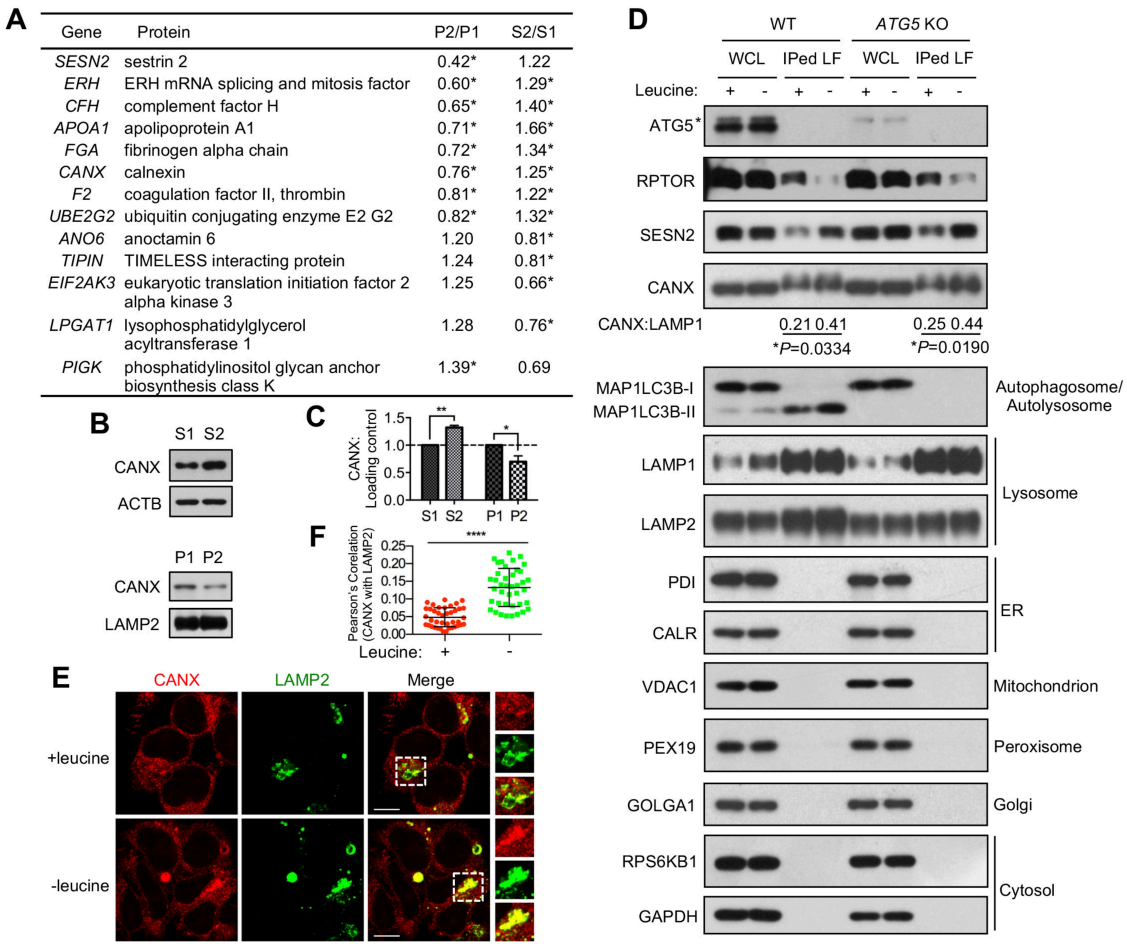

Figure 2. Identification of potential regulators from the leucine-stimulated MTORC1 cell-free system by comparative proteomics strategy. (A) From the MS dataset, the 13 proteins with fold change > 1.20 in P2/P1 (or S2/S1) and < 0.83 in S2/S1 (or P2/P1), with *P*-value < 0.05 in at least one group overlapped in S2/S1_Up and P2/P1_Down were listed in the table. (B) Immunoblotting of CANX (calnexin) in S1, P1, S2, P2 from the cell-free system. ACTB/β-Actin and LAMP2 were used as loading controls for supernatant and CLF, respectively. (C) Quantification of CANX:ACTB and CANX:LAMP2 in fractions as described in (A). Data are mean ± s.d. (n = 3 biological replicates). *$P < 0.05$, **$P < 0.01$ (Student's *t*-test). (D) Wild-type (WT) or *ATG5* knockout (KO) HEK293T cells transfected with 3× *HA*-tagged *TMEM192* plasmids were treated as indicated, and subjected to an immunoprecipitation-based lysosome capture process. The WCL and immunoprecipitated lysosome fractions (IPed LF) were immunoblotted for the level of the indicated proteins. Quantifications were performed with 3 replicates. *nonspecific band. (E) Leucine deprivation promoted CANX colocalization with LAMP2 in HEK293T cells. HEK293T cells were cultured with fresh complete or leucine-deprived media for 1 h, immunostained with antibodies against CANX (red) and LAMP2 (green), and observed with a laser scanning confocal microscope. Scale bar: 10 μm. (F) Quantification of the colocalization between CANX and LAMP2 using Pearson's Correlation Coefficient. Quantification was carried out on 40 cells. Data are mean ± s.d., ****$P < 0.0001$ (Student's *t*-test).

based lysosome capture method [28,29], we proved that leucine deprivation increased lysosome-associated abundance of SESN2 and CANX, but not the other ER markers PDI (protein disulfide isomerase) and CALR (calreticulin), in either wild-type (WT) or autophagy-deficient HEK293T cells, suggesting that 1) leucine deprivation specifically induced the lysosomal translocation of CANX but not other well-known ER markers; 2) the lysosomal translocation of CANX under leucine deprivation was autophagy-independent (Figure 2D). Moreover, *in vivo* immunostaining assays suggest that CANX colocalized with lysosomal membrane marker LAMP2 in HEK293T cells after leucine deprivation (Figure 2E and **2F**).

We next investigated whether CANX is involved in leucine-stimulated MTORC1 activity. We generated a *CANX* knockout (KO) HEK293T cell line by the CRISPR (clustered regularly interspaced short palindromic repeats)-Cas9 (CRISPR-associated protein 9) technology (Figure 3A) and confirmed the KO of *CANX* (Figure 3B; **Fig. S3A** and **S3B**). Compared to WT cells, *CANX* KO cells displayed MTORC1 activity insensitive to leucine deprivation, as indicated by phosphorylation of RPS6KB1, EIF4EBP1, ULK1, the common substrates of MTORC1 (Figure 3C and **3D**). Meanwhile, the relative abundance of autophagy indicator MAP1LC3B (microtubule associated protein 1 light chain 3 beta)-II [30] and the main autophagic substrate SQSTM1/p62 (Figure 3C and 3D), or the fluorescent dot number of endogenic MAP1LC3B (Figure 3E and 3F) were insensitive to leucine deprivation in *CANX* KO cells, suggesting that autophagy activity was also insensitive to leucine deprivation in *CANX* KO cells. However, the MTORC1 activity was still sensitive to serum starvation in *CANX* KO cells (**Fig. S3C** and **S3D**). Interestingly, in *CANX* KO cells, MTORC1 activity was insensitive to the deprivation of leucine or arginine, but not of lysine, suggesting that CANX is probably involved in other amino acids (but not all)-stimulated MTORC1 activation (**Fig. S3E**).

CANX regulates leucine-stimulated MTORC1 activity upstream of the RRAG GTPases

To investigate the relationship between the RRAG GTPases and CANX for MTORC1 regulation. We generated the *RRAGA RRAGB* double-KO (DKO) and *CANX RRAGA RRAGB* triple-KO (TKO) cell lines (**Fig. S4A**). In both *RRAGA RRAGB* DKO and *CANX RRAGA RRAGB* TKO cells, MTORC1 has low activity, and was insensitive to leucine deprivation (Figure 4A-4D). Meanwhile, autophagy activity was higher in both DKO and TKO cells than in *CANX* KO cells (**Fig. S4B** and **S4C**). In addition, introduction of the dominant-negative RRAG mutants ($RRAGB^{T54N}$ and

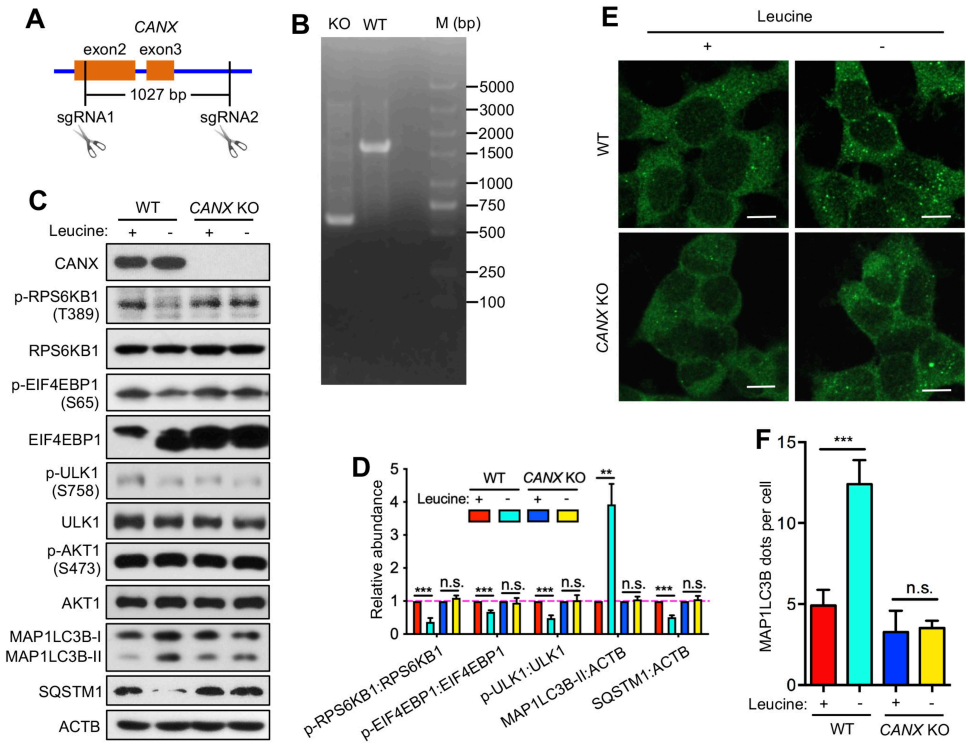

Figure 3. CANX is essential for the leucine-stimulated MTORC1 activity. (A) The strategy for the CRISPR/Cas9-mediated *CANX* KO using two pairs of single-guide RNAs (sgRNA1 and sgRNA2). (B) Validation of the KO of *CANX* by gel electrophoresis following the genomic PCR of specific *CANX* fragments, expected PCR products were 1591 bp for WT cells while ~584 bp for *CANX* KO cells. (C) The MTORC1 and autophagy activities were insensitive to leucine deprivation in *CANX* KO cells. WT or *CANX* KO HEK293T cells were cultured with fresh complete or leucine-deprived media for 1 h, cell lysates were immunoblotted for the level and phosphorylation abundance of the indicated proteins. (D) Quantification of the relative level and phosphorylation abundance of each protein. Data are mean ± s.d. (n = 3 biological replicates). $^{**}P < 0.01$; $^{***}P < 0.001$; n.s., not significant (Student's *t*-test). Note that all blots in the leucine deprivation group were normalized with their corresponding leucine supplementation group. (E) Cells were treated as (C), immunostained with antibody against MAP1LC3B, and visualized with confocal microscopy. Scale bar: 10 μm. (F) Quantification of MAP1LC3B dots in each immunostained cell as described in (E). Data are mean ± s.d. (n = 4 biological replicates). $^{***}P < 0.001$; n.s., not significant (Student's *t*-test).

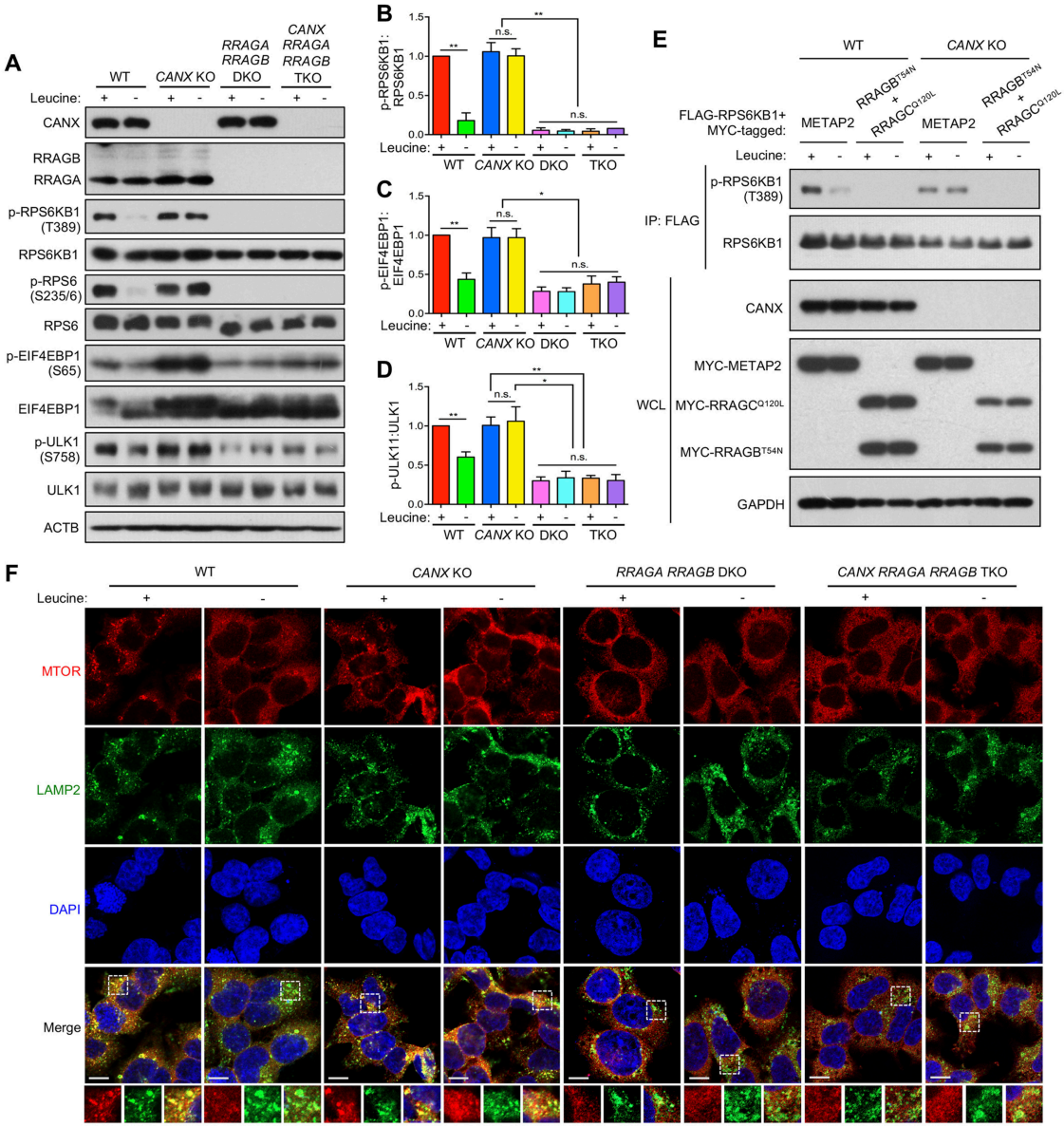

Figure 4. CANX regulates the leucine-stimulated lysosomal translocation of MTOR upstream of the RRAG GTPases. (A) WT, *CANX* KO, *RRAGA RRAGB* double-KO (DKO), and *CANX RRAGA RRAGB* triple-KO (TKO) HEK293T cells were cultured with fresh complete or leucine-deprived media for 1 h, the cell lysates were immunoblotted for the level and phosphorylation abundance of the indicated proteins. (B-D) Quantification of the relative phosphorylation abundance of RPS6KB1 (B), EIF4EBP1 (C), and ULK1 (D). Data are mean ± s.d. (n = 3 biological replicates). *$P < 0.05$; **$P < 0.01$; n.s., not significant (Student's *t*-test). (E) WT or *CANX* KO cell transfected with *FLAG*-tagged *RPS6KB1* and different *MYC*-tagged plasmids were treated as indicated, and immunoprecipitated with FLAG beads. The whole cell lysates (WCLs) and immunoprecipitates (IPs) were immunoblotted for the indicated proteins. Note that for the detection of p-RPS6KB1 signal, 10 times diluted WCLs were used. (F) WT, *CANX* KO, *RRAGA RRAGB* DKO, and *CANX RRAGA RRAGB* TKO HEK293T cells were cultured with fresh complete or leucine-deprived media for 1 h, immunostained with antibodies against MTOR (red) and LAMP2 (green), and co-stained with DAPI (blue) for DNA content. Scale bar: 10 μm. Quantification of the colocalization between MTOR and LAMP2 using Pearson's Correlation Coefficient were showed in **Fig. S4D.**

RRAGC^{Q120L}) strongly inhibited MTORC1 activity in either WT or *CANX* KO cells (Figure 4E). Moreover, in *CANX* KO cells, MTOR was constitutively localized on the lysosome in both normal and leucine deprivation conditions, while in *RRAGA RRAGB* DKO and *CANX RRAGA RRAGB* TKO cells, MTORC1 was barely localized to the lysosome in both normal and leucine deprivation conditions (Figure 4F; **Fig. S4D**). Together, these results indicate that the CANX acts upstream of the RRAG GTPases to regulate leucine-stimulated MTORC1 activity.

LAMP2 binds to CANX after leucine deprivation and regulates leucine-stimulated MTORC1 activity

Next, we aimed to explore if there was protein located onto the lysosomal membranes to act as a binding partner for CANX after leucine deprivation. By combining IP with MS analysis, we found that under leucine deprivation, both LAMP1 and LAMP2 were co-precipitated with CANX (Figure 5A; **Table S4**). However, it seems that the binding of LAMP1 to CANX was not leucine-sensitive, which was

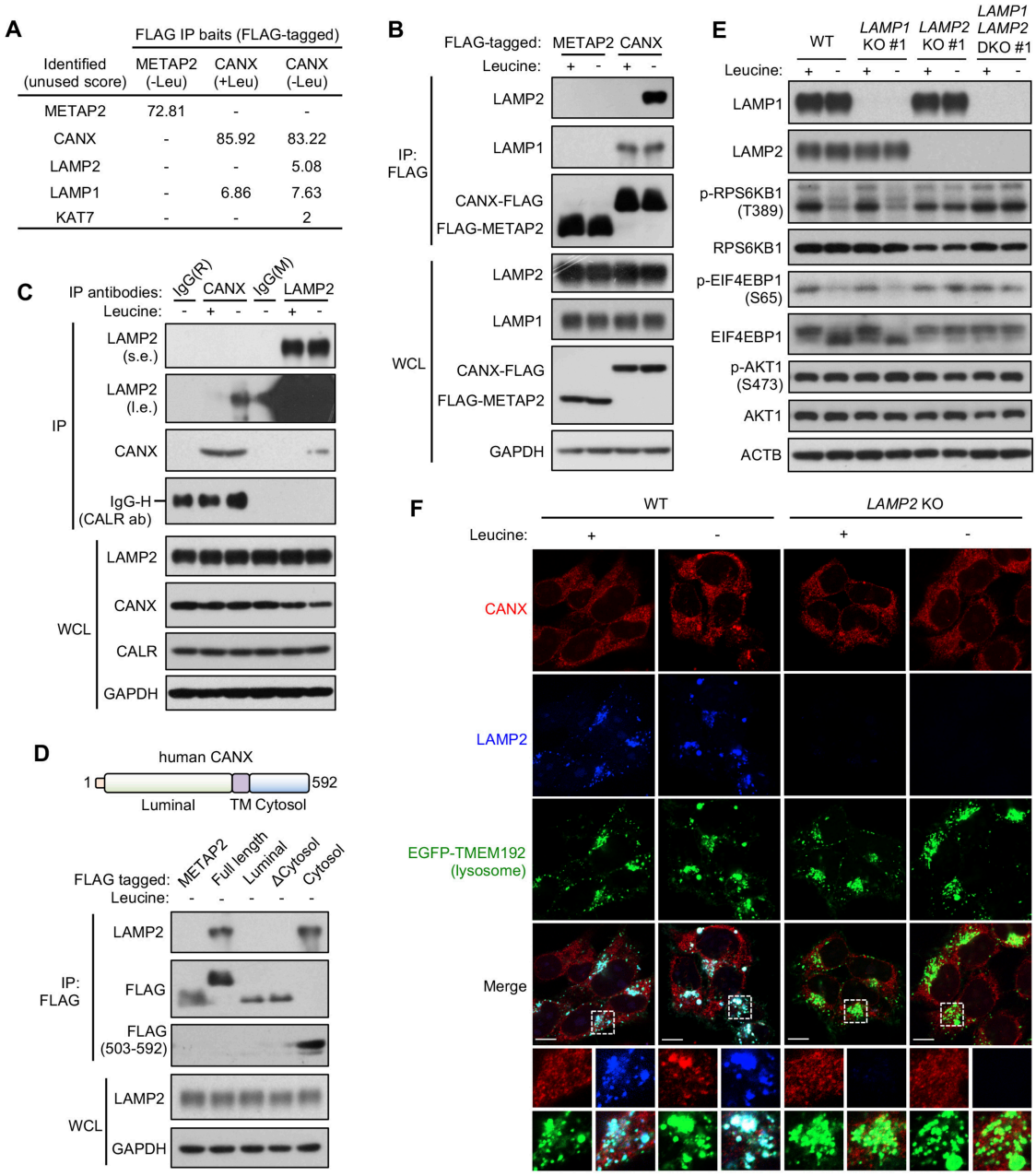

Figure 5. LAMP2 binds to CANX to regulate its lysosomal translocation after leucine deprivation. (A) FLAG immunoprecipitation (IP) combined with mass spectrometry (MS) analyses identified LAMP2 and KAT7 in the immunoprecititates from FLAG-tagged CANX after leucine deprivation (-Leu), but not leucine replete (+Leu) condition. The FLAG-tagged METAP2 is a negative control for the IP and MS assays. (B) Endogenous LAMP2 co-immunoprecipitated with exogenously expressed CANX after leucine deprivation. HEK293T cells were transfected with FLAG-tagged plasmids, treated as indicated, and immunoprecipitated with FLAG beads. The whole cell lysates (WCLs) and immunoprecipitates (IPs) were immunoblotted for the indicated proteins. (C) Endogenous CANX and LAMP2 interacted with each other after leucine deprivation. Cells were treated as indicated, and immunoprecipitated with the corresponding antibodies for the indicated proteins. The WCLs and IPs were immunoblotted for the indicated proteins. The isotype controls for antibodies CANX (rabbit monoclone) and LAMP2 (mouse monoclone) were rabbit IgG(R) and mouse IgG(M), respectively. s.e., short exposure, l.e., long exposure. Note that since the band position of CALR is very close to the IgG heavy chain, we are not confident if CALR is present in CANX IPs. (D) The cytosol part of CANX is sufficient for binding to LAMP2 after leucine deprivation. HEK293T cells transfected with plasmids expressing different FLAG-tagged fragments of CANX were cultured with leucine-deprived media for 1 h, and immunoprecipitated with FLAG beads. The whole cell lysates (WCLs) and immunoprecipitates (IPs) were immunoblotted for the indicated proteins. (E) The MTORC1 activity was insensitive to leucine deprivation in *LAMP2* KO cells, but not in *LAMP1* KO cells. WT, *LAMP1* KO, *LAMP2* KO, or *LAMP1 LAMP2* DKO HEK293T cells were cultured with fresh complete or leucine-deprived media for 1 h, cell lysates were immunoblotted for the level and phosphorylation abundance of the indicated proteins. (F) The CANX translocation to lysosomes induced by leucine deprivation was disrupted in *LAMP2* KO cells. WT and *LAMP2* KO cells transfected with EGFP-TMEM192 (another lysosome marker) were cultured with fresh complete or leucine-deprived media for 1 h, and immunostained with CANX (red) and LAMP2 (blue) antibodies. Scale bar: 10 µm.

supported by the observation that LAMP1 co-precipitated with CANX in either leucine replete or deprived condition (Figure 5A and **5B**). While both exogenous and endogenous CANX precipitated endogenous LAMP2 only after leucine deprivation (Figure 5B and **5C**). In addition, we found that the cytosol fragment of CANX was sufficient to mediate the binding of CANX to LAMP2 after leucine deprivation (Figure 5D). Most importantly, like in *CANX* KO cells, in *LAMP2* KO or *LAMP1 LAMP2* DKO, but not in *LAMP1* KO HEK293T cells, MTORC1 activity was insensitive to leucine deprivation (Figure 5E**; Fig. S5A**). Meanwhile, in *LAMP2* KO cells, the lysosomal translocation of MTOR was insensitive to leucine deprivation (**Fig. S5B** and **S5C**), and CANX did not colocalize with another lysosome marker TMEM192 (transmembrane protein 192) [29] under leucine deprivation (Figure 5F**; Fig. S5D**). These results suggest that LAMP2 acts as a binding partner of CANX on lysosomes after leucine deprivation and is essential for lysosomal translocation of CANX to regulate leucine-stimulated MTORC1 activity.

K525 crotonylation of CANX is essential for leucine-stimulated MTORC1 activity

PTMs often change the conformation and subcellular localization of proteins. Interestingly, recently we found that leucine deprivation significantly promoted the global lysine (K) crotonylation modification, but not K acetylation, ubiquitination, or succinylation, of proteome in mouse primary hepatocyte cell line AML12 (unpublished data). Via a K crotonylation proteomics analysis (raw data are available in ProteomeXchange Consortium with data set identifier PXD018118), we found that the crotonylation modification of CANX at K90 and K526 might be upregulated after leucine deprivation in AML12 cells (Figure 6A-6C). Further IP analysis using Pan-K crotonylation (Kcr) antibody validated that the crotonylation of CANX was increased under leucine deprivation condition in AML12 cells (Figure 6D). Also, leucine deprivation significantly decreased the MTORC1 activity in AML12 cells (**Fig. S6A** and **S6B**). This drives us to explore if CANX crotonylation is involved in the regulation of leucine-stimulated MTORC1 in HEK293T cells. Indeed, in HEK293T cells, leucine deprivation increased the abundance of crotonylation of CANX, which was verified by endogenous IP assays using antibodies against Pan-Kcr or CANX (Figure 6D and 6E), as well as exogenous FLAG IP for FLAG-tagged CANX (Figure 6F). Interestingly, although both arginine and leucine regulated MTORC1 through CANX (**Fig. S3E**), arginine deprivation did not obviously change the CANX Kcr abundance (**Fig. S6C**). Importantly, mutant of K525R (lysine to arginine at residue 525) and K89R+K525R, but not K89R alone or WT CANX, still rendered MTORC1 activity insensitive to leucine deprivation in *CANX* KO HEK293T cells (Figure 6G**; Fig. S6D**), suggesting that the K525 site, but not K89, of CANX is crucial for leucine-stimulated MTORC1 activity. In addition, CANX mutant K525R was hindered to translocate to the lysosome after leucine deprivation (**Fig. S6D-S6E**). Importantly, the K525R mutant displayed no differential crotonylation abundance after leucine deprivation, but WT CANX did (Figure 6H), suggesting that the K525 is the crotonylation site affected by leucine deprivation. In addition, CANX mutant K525R did not bind to LAMP2 after leucine deprivation (Figure 6H). Together, these results demonstrate that the K525 crotonylation of CANX is essential for leucine-stimulated MTORC1 activity.

KAT7 mediates the K525 crotonylation of CANX to regulate the leucine-stimulated MTORC1 activity

We next questioned which enzyme(s) mediates the crotonylation of CANX under leucine deprivation. Given that currently all known crotonylation-mediated enzymes (e.g., EP300, CREBBP [CREB binding protein], KAT2B [lysine acetyltransferase 2B], KAT8) belong to acetyltransferase (**Fig. S7A**) [31–33], we scanned the CANX IP MS data with "acetyltransferase". We found that a lysine acetyltransferase, KAT7, co-precipitated with CANX under leucine deprivation, but not leucine replete condition (Figure 5A**; Table S4**). Indeed, FLAG-tagged CANX precipitated endogenous KAT7, but not KAT8, after leucine deprivation (Figure 7A). Endogenous IP confirmed that CANX and KAT7 (but not KAT8) precipitated with each other under leucine deprivation condition (Figure 7B). Mutant of K525R did not precipitate KAT7 in *CANX* KO cells, but WT CANX did, suggesting that KAT7 directly binds to the K525 of CANX (Figure 7C). More importantly, an *in vitro* crotonylation assay by incubating purified GST (glutathione S-transferase)-KAT7 with WT GST-CANX or GST-CANX K525R mutant confirmed that KAT7 directly crotonylated WT CANX, but not CANX K525R mutant (Figure 7D). In *KAT7* KO cells (**Fig. S7B**), CANX did not bind to LAMP2 after leucine deprivation, but in *LAMP2* KO cells, CANX still precipitated KAT7 (Figure 7E), suggesting that KAT7 binds to CANX upstream of LAMP2 after leucine deprivation. In addition, in *KAT7* KO cells, MTORC1 activity was also insensitive to leucine deprivation (Figure 7F**; Fig. S7C**). While the MTOR translocation to the lysosome was also insensitive to leucine deprivation (Figure 7G and **7H**). Moreover, leucine deprivation-induced CANX translocation to the lysosome was disrupted in *KAT7* KO cells (**Fig. S7D** and **S7E**). The KAT7 abundance was higher in nucleus than in cytoplasm but was not differential in nuclear or cytoplasmic compartments between leucine replete and deprived conditions in both HEK293T (Figure 7I and **7J**) and AML12 cells (**Fig. S7F** and **S7G**), suggesting that KAT7 unlikely translocated from nucleus to cytoplasm after leucine deprivation. Taken together, the above results suggest that KAT7 directly binds to and crotonylates CANX at its K525 site after leucine deprivation, which controls the CANX translocation to lysosomes and regulates MTORC1 activity.

CANX regulates Ragulator and RRAG GTPases interaction through LAMP2

Next we aimed to determine whether the leucine-sensitive CANX-LAMP2 complex was associated with any known MTORC1 regulatory mechanism. By combining

A

Accession	Gene name	WCL protein ratio (-Leu:Normal)	Normalized Kcr Ratio (-Leu:Normal)	Normalized *P* value	Position	Amino acid	PEP	Score	Charge	Mass error [ppm]
P35564	*Canx*	1.061 ± 0.027	5.684 ± 0.083	6.37E-08	90	K	0.000792	92.19	3	0.071399
			6.011 ± 0.266	4.19E-05	526	K	0.00154	44.788	4	0.38462

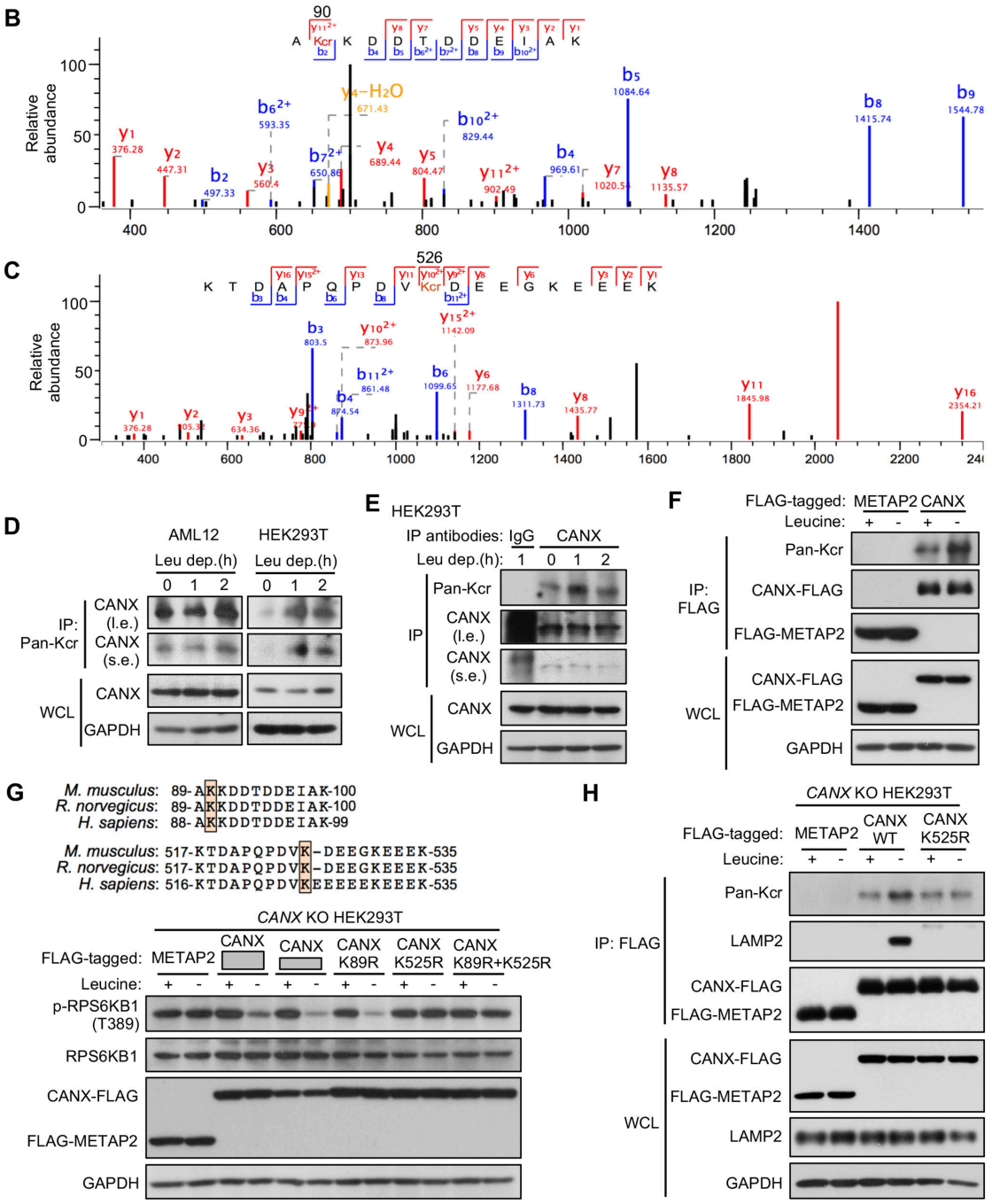

Figure 6. The K525 crotonylation of CANX is essential for leucine-stimulated MTORC1 activity. (A) The crotonylation levels of sites lysine (K) 90 and K526 of CANX were upregulated after leucine deprivation in AML12 cells. Original MS data to generate this result are from ProteomeXchange Consortium (dataset identifier: PXD018118). (B and C) The MS/MS spectra of K90 (B) and K526 (C) crotonylation of CANX derived from liquid chromatography (LC)-MS/MS analysis. Original MS data to generate these results are from ProteomeXchange Consortium (dataset identifier: PXD018118). (D) CANX crotonylation was increased after leucine deprivation in both AML12 and HEK293T cells. AML12 and HEK293T cells were cultured with leucine-deprived media for 0, 1, or 2 h, and immunoprecipitated with a pan-Kcr antibody against crotonylated-lysine proteins. The WCLs and IPs were immunoblotted with indicated antibodies. (E) HEK293T cells were cultured with leucine-deprived media for 0, 1, or 2 h, and immunoprecipitated with antibody against CANX. The WCLs and IPs were immunoblotted with indicated antibodies. (F) The crotonylation of exogenously expressed CANX was increased after leucine deprivation. HEK293T cells were transfected with FLAG-tagged plasmids, treated as indicated, and immunoprecipitated with FLAG beads. The WCLs and IPs were immunoblotted with indicated antibodies. (G) The knockin of CANX mutant K525R or K89R+K525R did not rescue the MTORC1 sensitivity to leucine deprivation in *CANX* KO HEK293T cells, while the knockin of WT or K89R mutant did. *CANX* KO cells with knockin of indicated WT or mutant plasmids were cultured with fresh complete or leucine-deprived media for 1 h, cell lysates were immunoblotted for the level and phosphorylation abundance of the indicated proteins. Note that the residues K90 and K526 of CANX in mouse were corresponding to K89 and K525 of CANX in human. (H) Leucine deprivation induced crotonylation of CANX at K525, and CANX mutant K525R did not bind to LAMP2 under leucine deprivation. *CANX* KO HEK293T cells were transfected with indicated FLAG-tagged plasmids, cultured with fresh complete or leucine-deprived media for 1 h, and immunoprecipitated with FLAG beads. The WCLs and IPs were immunoblotted for the indicated proteins. Data (D-F, H) are representative of two independent experiments.

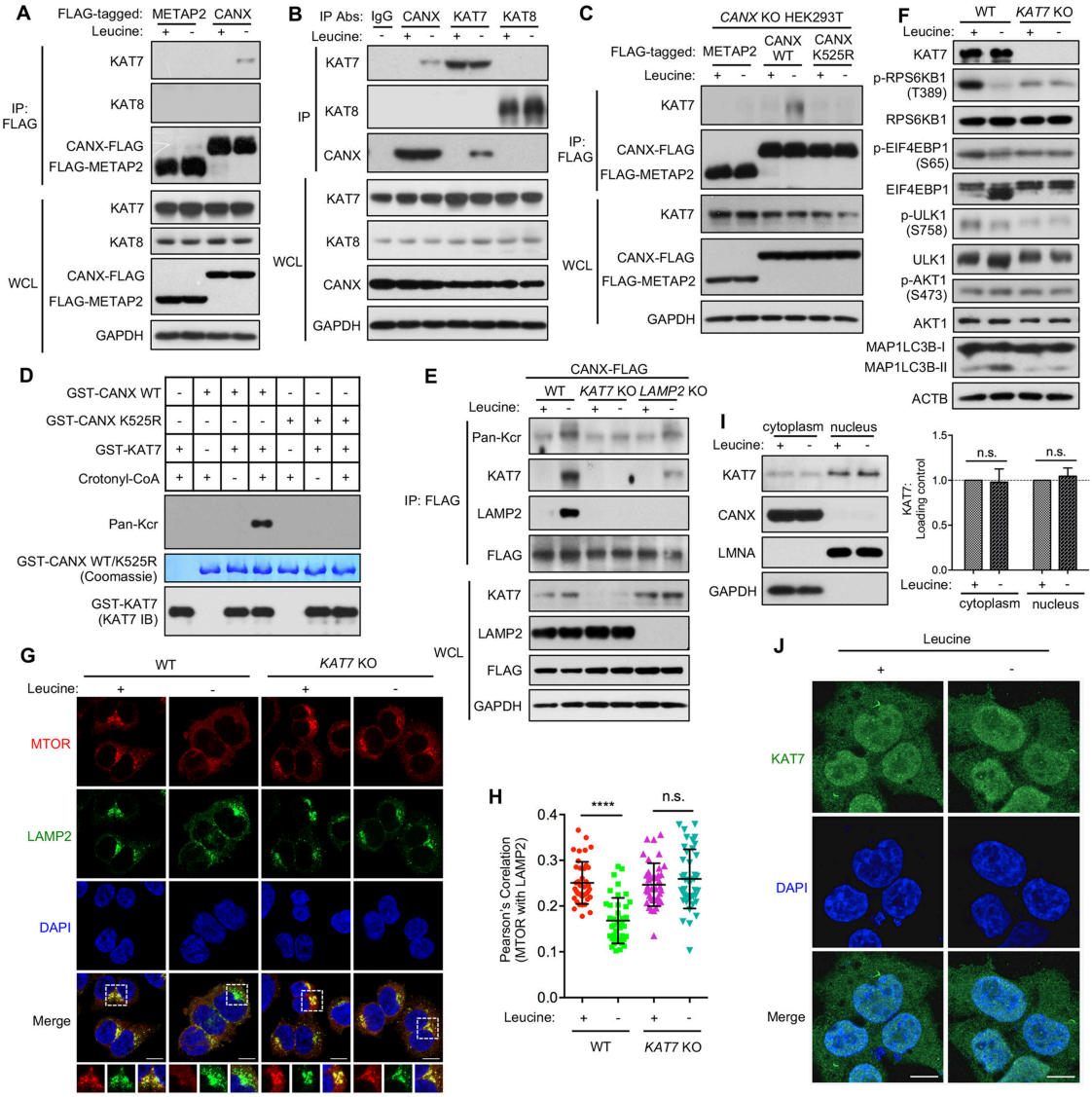

Figure 7. KAT7 mediates the K525 crotonylation of CANX after leucine deprivation. (A) Endogenous KAT7, but not KAT8, co-immunoprecipitated with exogenously expressed CANX after leucine deprivation. HEK293T cells were transfected with FLAG-tagged plasmids, treated as indicated, and immunoprecipitated with FLAG beads. The WCLs and IPs were immunoblotted for the indicated proteins. (B) Endogenous KAT7 (but not KAT8) and CANX interacted with each other after leucine deprivation. Cells were treated as indicated, and immunoprecipitated with the corresponding antibodies. The WCLs and IPs were immunoblotted for the indicated proteins. (C) KAT7 interacted with CANX at K525 of CANX under leucine deprivation. *CANX* KO HEK293T cells were transfected with indicated FLAG-tagged plasmids, cultured with fresh complete or leucine-deprived media for 1 h, and immunoprecipitated with FLAG beads. The WCLs and IPs were immunoblotted for the indicated proteins. (D) *In vitro* crotonylation assays using purified GST-CANX WT or GST-CANX K525R, and GST-KAT7. (E) KAT7 interacted with CANX upstream of LAMP2 after leucine deprivation. WT, *KAT7* KO, or *LAMP2* KO cells transfected with FLAG-tagged CANX were cultured with fresh complete or leucine-deprived media for 1 h, and immunoprecipitated with FLAG beads. The WCLs and IPs were immunoblotted for the indicated proteins. (F) MTORC1 and autophagy activities were insensitive to leucine deprivation in *KAT7* KO cells. WT or *KAT7* KO HEK293T cells were cultured with fresh complete or leucine-deprived media for 1 h, cell lysates were immunoblotted for the level and phosphorylation abundance of the indicated proteins. (G) The lysosomal translocation of MTOR was insensitive to leucine deprivation in *KAT7* KO cells. WT and *KAT7* KO cells were cultured with fresh complete or leucine-deprived media for 1 h, immunostained with MTOR (red) and LAMP2 (green) antibodies, and co-stained with DAPI (blue) for DNA content. Scale bar: 10 μm. (H) Quantification of the colocalization between MTOR and LAMP2 using Pearson's Correlation Coefficient. Quantification was carried out on 40 cells. Data are mean ± s.d. ****$P < 0.0001$; n.s., not significant (Student's *t*-test). (I) HEK293T cells cultured with fresh complete or leucine-deprived media were fractionated into nuclear and cytoplasmic fractions, which were immunoblotted for the indicated proteins. LMNA and GAPDH were used as indicators for nuclear and cytoplasmic fractions, respectively. Quantification of the relative abundance of KAT7 from three biological replicates was shown in the bottom, n.s., not significant (Student's *t*-test). (J) HEK293T cells cultured with fresh complete or leucine-deprived media were immunostained with antibody against KAT7, and visualized with confocal microscopy. Scale bar: 10 μm. Data (A-E) are representative of two independent experiments.

crosslinking with IP strategy, we found that leucine deprivation promoted CANX interaction with the v-ATPase and Ragulator components ATP6V1B2 and LAMTOR1, but not other known regulators including SESN2, LARS, GATOR2 (indicated by MIOS), GATOR1 (indicated by NPRL3), and RRAG GTPases (indicated by RRAGA) (Figure 8A). LAMP2 was required for the leucine deprivation-induced interaction of CANX with the v-ATPase-Ragulator complex, which was indicated by the dramatically decreased interaction of CANX with v-ATPase and Ragulator in *LAMP2* KO cells (Figure 8B). More importantly, CANX loss disrupted the leucine deprivation-induced interaction of Ragulator (LAMTOR1) with RRAG GTPases (RRAGA), but had no effect on the interaction of GATOR1 (NPRL2)

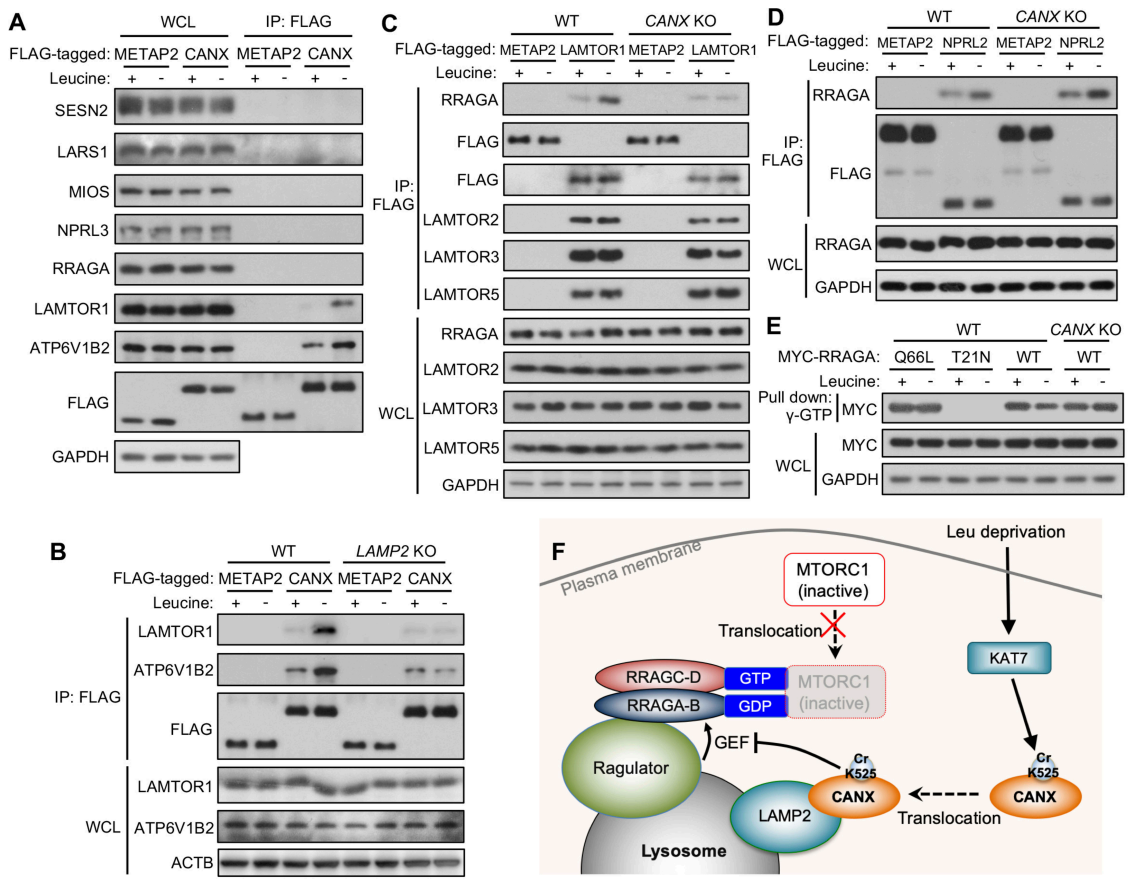

Figure 8. CANX interacts with v-ATPase/Ragulator in a leucine-sensitive manner and the interaction requires LAMP2. (A) HEK293T cells were transfected with FLAG-tagged plasmids, treated as indicated, and crosslinked with DSP before subjected to immunoprecipitation with FLAG beads. The WCLs and IPs were immunoblotted for the indicated proteins. (B) WT or *LAMP2* KO HEK293T cells were transfected with FLAG-tagged plasmids, treated as indicated, and crosslinked with DSP before subjected to immunoprecipitation with FLAG beads. The WCLs and IPs were immunoblotted for the indicated proteins. (C and D) WT or *CANX* KO HEK293T cells were transfected with FLAG-tagged plasmids, treated as indicated, and crosslinked with DSP before subjected to immunoprecipitation with FLAG beads. The WCLs and IPs were immunoblotted for the indicated proteins. (E) WT or *CANX* KO HEK293T cells were transfected with MYC-tagged WT or mutated *RRAGA* plasmids, treated as indicated, and pull-down was performed with γ-Amino-hexyl-GTP agarose beads. The WCLs and pull-down products were immunoblotted for the indicated proteins. (F) Schematic depiction of this study. Leucine deprivation promotes KAT7-mediated crotonylation of CANX at K525. The crotonylated CANX translocates to the lysosome surface, where CANX binds to LAMP2, and inhibits the Ragulator activity toward RRAGA, thus resulting the decreased lysosomal translocation of MTOR. Data (A-E) are representative of two independent experiments.

with RRAG GTPases (Figure 8C and 8D). CANX loss did not affect the complex stability of Ragulator (Figure 8C). While in *CANX* KO cells, RRAGA-GTP level was increased even under leucine deprived condition (Figure 8E). These results suggest that CANX likely regulates MTORC1 activity through disturbing the GEF activity of Ragulator toward RRAGA.

Discussion

In addition to acting as building blocks for protein synthesis, some amino acids also play multifunction in a number of biological processes. Branched-chain amino acids, especially leucine, have been characterized as functional amino acids that improve malnutrition by regulating the MTORC1 and autophagy pathways [24]. For MTORC1 pathway, there are some sensors, including LARS [34] and recently identified SESN2 [35], signal the intracellular leucine level to MTORC1 and regulate the activity of MTORC1, which needs MTORC1 itself to be recruited to the lysosome surface. Given that a series of regulators for the amino acids (leucine)-stimulated MTORC1 pathway have been identified continuously, whether there are more is an important question going forward. A proteomics scale screening is a helpful approach to provide us the reference for identification of unknown regulators. In the present study, we for the first time combined the *in vitro* reconstitution with comparative proteomics technology to screen potential regulators in the leucine-stimulated MTORC1 pathway. Our results demonstrate that leucine deprivation promotes the KAT7-mediated K525 crotonylation of CANX, which translocates to the lysosome surface to bind to LAMP2 and regulate the interaction of the v-ATPase-Ragulator complex with RRAG GTPases, and inhibits the lysosomal translocation of MTOR, thus resulting the decreased MTORC1 activity (Figure 8F).

CANX is a highly abundant transmembrane protein that is located in the ER (endoplasmic reticulum) membrane [36]. Previous study has implicated that CANX is involved in autophagy regulation [27], although the mechanism has not

been fully elucidated. Recently, by using a combination of immunocapture of lysosomes with proteomics strategy, a study has showed that CANX exists in the lysosomal proteome [28]. In the present study, proteomics data together with immunoblotting assays indicated that amino acids (leucine) deprivation promoted the abundance of CANX connected with the lysosome. In addition, by using another well-established immunoprecipitation-based lysosome capture method, we also proved that leucine deprivation specifically induced the lysosomal translocation of CANX, but not the other ER markers PDI and CALR, in an autophagy-independent manner. We also proved that CANX, at least in part, colocalized with lysosome markers LAMP2 and TMEM192. Moreover, CANX directly bound to lysosomal marker LAMP2 through its cytosol part after leucine deprivation. These findings suggest that CANX indeed translocated to lysosomes after leucine deprivation. Moreover, further functional assays showed that *CANX* loss-of-function significantly rendered MTORC1 signaling insensitive to leucine deprivation, indicating that CANX is an essential regulator for the leucine-stimulated MTORC1 pathway. Interestingly, a previous study has found that CANX colocalized with MTOR [37], suggesting that 1) MTORC1 was activated on the ER, or 2) ER-located CANX was present in other subcellular region(s) where MTORC1 was activated. Since many later studies have elucidated that MTORC1 is mainly activated on the lysosome by directly binding to the RRAG GTPases and RHEB GTPase, we could infer that the second one is more likely to happen. Given that the cytosol part of ER lumen-resident CANX plays crucial roles in some intracellular signaling pathways by binding to specific partner [38], we reasoned that it is likely that under leucine-deprived condition, the cytosolic fragment of the ER lumen-resident CANX might be recruited to lysosomes to regulate the lysosomal translocation of MTOR. Importantly, the interaction of CANX and LAMP2 suggests that the crosstalk of ER and lysosome, which has been observed visually [39], might play crucial roles in regulating some signaling pathways including the MTORC1 pathway. In support of this notion, two recent studies have proved that ER-lysosome contacts played fundamental roles in glucose and cholesterol sensing, which are mediated by ER-located calcium protein TRPV (transient receptor potential channel subfamily V) and VAPA (VAMP associated protein A)-VAPB, respectively [40,41].

Another interesting finding is that KAT7-mediated crotonylation of CANX is involved in the regulation of leucine-stimulated MTORC1 activity. After identified in 2011 [42], lysine crotonylation modifications were largely investigated on nuclear histones [31,42,43], suggesting its crucial roles in epigenetic regulation of gene expression. However, two recent global profiling study reported that a large amount (35.7% and 40%, respectively) of crotonylated proteins were located in cytoplasm [32,44], highlighting the potential roles of crotonylation modification in regulating various cellular processes besides epigenetic regulation. Our study, for the first time, connects the non-histone protein crotonylation modification with regulation of one of the most important cellular metabolic pathways-MTORC1. We showed that the K525 crotonylation of CANX was essential for leucine-stimulated MTORC1 activity. The subcellular locations of proteins are often changed by PTMs, such as phosphorylation [45,46], and acetylation [47], we found that the CANX mutant K525R did not bind to LAMP2 after leucine deprivation, suggesting that K525 crotonylation status controls the subcellular translocation of CANX. Since the activation of MTORC1 involves lysosomal translocation of MTORC1 itself as well as a series of regulators, while the roles of PTMs in these translocation events have been less explored. Our study thus provides new insights into the regulation of MTORC1 by PTMs, especially the newly identified ones such as propionylation, succinylation, and crotonylation [20]. Typically, PTMs are mediated by the associated enzymes, suggesting that many enzymes are likely to play roles in the processes that are regulated by their substrates. In the current study, we identified KAT7 as a responsible enzyme for the K525 crotonylation of CANX. The KAT7-mediated CANX K525 crotonylation was significantly upregulated under leucine deprivation, which is probably caused by two reasons: 1) leucine deprivation might upregulate the abundance of crotonyl-CoA, the substrate for protein crotonylation, and/or 2) leucine deprivation might alter the activity of KAT7. Generally, the cellular crotonyl-CoA is derived from the crotonate or breakdown of long-chain fatty acids via β-oxidation [20]. Interestingly, despite the mechanism currently unknown, we have found that leucine deprivation activates fatty acid β-oxidation pathway in hepatocytes [48]. Thus, it is possible that leucine deprivation upregulates intracellular crotonyl-CoA by activating the fatty acid β-oxidation. In addition, consistent with previous report [49], we found that KAT7 existed in both nucleus and cytoplasm. Unlike EP300, which was found to translocate from nucleus to cytoplasm after re-stimulated with leucine [18], we did not find any differential abundance of KAT7 in nuclear or cytoplasmic fractions of both AML12 and HEK293T cells after leucine deprivation, combined with the evidence that CANX only exists in cytoplasmic fractions, these results suggest that the KAT7-mediated crotonylation of CANX was likely independently happened in cytoplasm, which does not involve the translocation of KAT7 between nucleus and cytoplasm.

In summary, we identify CANX as an essential regulator for leucine-stimulated MTORC1 activity. Upon leucine deprivation, CANX is crotonylated by KAT7 and subsequently translocates to the lysosome and binds to LAMP2, which is required for CANX interaction with v-ATPase/Ragulator complex. The interaction of CANX with Ragulator regulates the binding of Ragulator to RRAG GTPases, inhibits Ragulator GEF activity toward RRAGA, resulting the decreased RRAGA-GTP level, finally impaired lysosomal translocation and activity of MTORC1. Although the detailed mechanism by which CANX altered the Ragulator GEF activity is still needed to be addressed in future explorations, our study provides a novel mechanism by which leucine regulates MTORC1 activity and may help identify potential pharmacological targets to deal with MTORC1-associated diseases.

Materials and methods

Antibodies and regents

Antibodies against ACTB/β-Actin (4967), RRAGA (4357), ATG5 (8540), RPTOR/Raptor (2280), PDI (3501), CALR/calreticulin (12,238), RPS6KB1/S6K1 p-T389 (9234), EIF4EBP1 p-S65 (9451), ULK1 (8054), ULK1 p-S757 (14,202), RPS6 p-S235/236 (4858), AKT1 p-S473 (4060), MIOS (13,557), LAMTOR2/p14 (8145), LAMTOR3/MAPKSP1 (8168), FLAG (14,793, for WB and immunostaining), CANX (2679, for IP and immunostaining), MTOR (2983, for immunostaining), rabbit isotype control (2729), and HRP-labeled anti-mouse secondary antibody (7076) were from Cell Signaling Technology; antibodies against FLAG (F3165), NPRL3 (HPA011741), MAP1LC3B (L7543), MYC (M4439), HRP-labeled anti-rabbit secondary antibody (A9169) were from Sigma; antibodies against LAMP1 (sc-20,011), LAMP2 (sc-18,822, for WB, IP and immunostaining), LMNA (sc-56,137), GOLGA1 (sc-59,820), AKT1 (sc-5298), RPS6 (sc-74,459), HA (sc-7392) were from Santa Cruz Biotechnology; antibodies against RRAGC (26,989-1-AP), VDAC1 (55,259-1-AP), EIF4EBP1 (60,246-1-Ig), GAPDH (60,004-1-Ig), KAT7 (13,751-1-AP), KAT8 (13,842-1-AP), SQSTM1/p62 (18,420-1-AP), SESN2 (10,795-1-AP), ATP6V1B2 (15,097-1-AP), LARS1 (21,146-1-AP), LAMTOR5/HBXIP (14,492-1-AP), MAP1LC3B (14,600-1-AP, for immunostaining) were from ProteinTech; antibodies against LAMTOR1/p18 (A11619), RPS6KB1 (A2190), CANX (A0803), mouse isotype control (AC011) were from ABclonal Technology; the antibody against lysine crotonylation (Pan-Kcr, PTM-502) were from PTM Biolabs; goat anti-mouse IgG (H + L) Alexa Fluor 350 (A21049), Alexa Fluor 488 (A11029), and goat anti-rabbit IgG (H + L) Alexa Fluor 488 (A11034), Alexa Fluor 594 (A11037) were from ThermoFisher Scientific. Anti-HA Agarose (A2095) and Anti-FLAG M2 affinity gel (A2220) were from Sigma; Anti-HA magnetic beads (88,837) were from ThermoFisher Scientific; Immobilized γ-Amino-hexyl-GTP beads (AC-117) were from Jena Bioscience; Protein A/G PLUS-Agarose (sc-2003) was from Santa Cruz Biotechnology. RPMI 1640 without amino acids (R8999-04A), or without glutamine and leucine (R8999-03) were from US Biologicals, RPMI 1640 without leucine, arginine, lysine was purchased from Sigma (R1780). Fetal bovine serum (FBS, 10,099) and Dulbecco's modified Eagle's medium (DMEM, C11995) were from Gibco. Arginine, glutamine, lysine, and leucine were purchased from Sigma. Dialyzed FBS (dFBS, 04–011-1) was from Biological Industries. All the restricted enzymes were from Takara except the *Bbs*I was from New England Biolabs.

Cell lines and culture

Human embryonic kidney 293 T (HEK293T) cells were provided by Jingjing Tong (Wuhan University, China), the *ATG5* knockout HEK293T cell line was a kind gift from Prof. Jun Cui (Sun Yat-sen University, China), and the mouse primary hepatocyte cell line AML12 [50] was a kind gift from Prof. Rui Zhou (Wuhan University, China). All cell lines were validated to be free of mycoplasma contamination. All cells were cultured in DMEM supplemented with 10% FBS and 1% penicillin-streptomycin at 37°C under 5% CO_2.

Amino acid-deprived media

To generate media without all amino acids, RPMI 1640 without amino acids was supplemented with 10% dFBS. To generate leucine or glutamine-deprived media, RPMI 1640 without leucine and glutamine was supplemented with 0.3 g/L glutamine or 0.05 g/L leucine (with the same concentration in full RPMI 1640 media), and 10% dFBS. To generate arginine or lysine-deprived media, RPMI 1640 without leucine, arginine, and lysine was supplemented with leucine (0.05 g/L) and lysine (0.04 g/L), or leucine (0.05 g/L) and arginine (0.2 g/L), with 10% dFBS. The control complete media for amino acid starvation assays was complete RPMI 1640 (US Biologicals, R8999) supplemented with 10% dFBS.

Preparation of lysosome and cytosol fractions for cell-free assays

HEK293T cells with 80 ~ 90% confluence were cultured in fresh complete or amino acid-deprived media for 1 h at 37°C under 5% CO_2. Then all cells (~$6x10^8$ cells) were harvested, collected by centrifugation (1,000 x g for 10 min at 4°C). After washed with ice-cold PBS (Hyclone, SH30256.01) twice, the suspension was centrifuged (1,000 x g for 5 min at 4°C) and the cell pellets were induced with a commercial lysosome isolation kit (Sigma, LYSISO1) to get the lysosome fraction (CLF) from the complete (CLF(+)) or amino acid-deprived (CLF(-)) media-cultured HEK293T cells following the manufacturer's protocol. Briefly, cells were resuspended in extraction buffer, and broken with a Dounce homogenizer (25 strokes). The homogenates were centrifuged at 2,000 x g for 10 min at 4°C, while the supernatants were collected and centrifuged at 20,000 x g for 20 min at 4°C. The resulting pellets were diluted with a 19% Optiprep Density Gradient Media Solution (supplied in the kit), the fractions were collected and centrifuged at 100,000 x g for 8 h at 4°C. The obtained fractions were incubated with 8 mM $CaCl_2$ for 15 min, and centrifuged at 5,000 x g for 15 min at 4°C. The resulting supernatants containing purified lysosomes were divided into 20 μl aliquots and tested for purity of lysosomes before applied for further assays. To prepare cytosol S100 fractions, HEK293T cells were grown to 80 ~ 90% confluence, the media was changed into fresh complete or amino acid-deprived media. After incubation for 1 h at 37°C under 5% CO_2, all cells were harvested, collected by centrifugation (1,000 x g for 10 min at 4°C). The cell pellets were washed twice with ice-cold PBS and resuspended in 5 volume of ice-cold fractionation buffer (50 mM KCl, 90 mM K-gluconate [Sango Biotech, A507810], 1 mM EGTA [Sango Biotech, A600077], 5 mM $MgCl_2$, 50 mM sucrose [Sango Biotech, A610498], 20 mM HEPES [Sigma, H3375] pH 7.4, supplemented with 2.5 mM ATP [Sango Biotech, A600311], 5 mM glucose [Sango Biotech, A501991] and protease inhibitors [Roche, 04693159001]). After incubation on ice for 30 min, the cells were then broken by passing 15 times through a G22 needle. After centrifugation for 10 min, the supernatants were

further centrifuged at 100,000 x g for 45 min at 4°C in an ultracentrifuge. The resulting supernatants (S100) from fresh complete (S100(+)) or amino acid-deprived (S100(-)) media-cultured cells were divided into 50 µl aliquots and stored at −80°C until used for the *in vitro* cell-free assays.

Recombinant protein purification for cell-free assays

To purify the recombinant HA-RPTOR protein, HEK293T cells were transfected with the recombinant plasmid for 24 h. After transfection, cells were harvested, washed once with ice-cold PBS, and lysed for 15 min on ice in lysis buffer (50 mM Tris-HCl, pH 8.0, 150 mM NaCl, 1 mM EDTA, 1% Triton X-100 [Santa Cruz Biotechnology, sc-29112A], protease inhibitor mixture), and centrifuged for 10 min at 14,000 x g at 4°C. The supernatants were added to 50% slurry of anti-HA agaroses that were pre-washed with lysis buffer 3 times. After 3 h incubation with gentle rotation at 4°C, the beads were centrifuged and washed with lysis buffer containing 500 mM NaCl 5 times. The beads were then incubated with 100 µg/mL HA peptide (Sigma, I2149) for 1 h at 4°C with gentle rotation. The resulting elutes were tested for purity with Coomassie Brilliant Blue and immunoblotting before used for the *in vitro* cell-free assays.

Cell-free assays

The prepared CLF (20 µl aliquots) was incubated with 0.1 µg purified HA-RPTOR, 50 µl S100 aliquots, and fractionation buffer (50 mM KCl, 90 mM K-gluconate, 1 mM EGTA, 5 mM $MgCl_2$, 50 mM sucrose, 20 mM HEPES, pH 7.4, supplemented with 2.5 mM ATP, 5 mM glucose and protease inhibitors), 250 µM GTP [Sigma, G8877], 100 µM GDP [Sigma, G7127] in a final volume of 100 µl at 37°C for each sample. After incubation for 30 min, the reaction tubes were transferred on ice to terminate the reaction, and subsequently centrifuged (17,800 x g, 4°C, 15 min) to separate the lysosome-enriched fractions from soluble proteins. The pellets were immunoblotted with anti-HA antibody to detect the binding of RPTOR and CLF, LAMP2 was used as loading control for RPTOR-lysosome association assays.

ITRAQ analysis

The amino acid-deprived CLF (CLF(-)) was incubated with HA-RPTOR, amino acid-deprived S100(-) and fractionation buffer, with (+Leu) or without (Control) 10 mM leucine supplementation. Each sample was in a final volume of 100 µl. After incubation for 30 min at 37°C, the reaction tubes were transferred on ice to terminate the reaction, and then centrifuged (17,800 x g) at 4°C. The resulting supernatants and pellets were applied to proteomics analysis.

Prepared samples were freeze-dried and dissolved with L3 dissolution buffer and cold acetone containing 10 mM DTT for 2 h. After centrifugation (15,871 x g) for 20 min at 15°C, the precipitates were collected and mixed with 800 µl cold acetone containing 10 mM DTT for 1 h at 56°C to break the disulfide bonds of proteins. After another centrifugation (15,871 x g) for 20 min at 15°C, the precipitates were collected and dried. For each sample, ~ 100 µg protein was dissolved with dissolution buffer in a final volume of 500 µl, and then diluted with 500 µl 50 mM NH_4HCO_3. After being reduced and alkylated, the samples were digested by adding 2 µg trypsin for incubation overnight at 37°C. After incubation, equal volume of 0.1% FA was added for acidizing and the peptides were passed through a Strata-X C18 pillar for three times, washed with 0.1% FA plus 5% ACN twice, and eluted with 1 ml 0.1% FA plus 80% ACN. The eluted peptides were dried with a vacuum concentration meter, and re-dissolved in 20 µl 0.5 M TEAB for labeling. Samples were labeled with the iTRAQ reagents (AB Sciex U.K. Limited) below: supernatant in Control (S1), 113; pellet in Control (P1), 114; supernatant in +Leu (S2), 115; pellet in +Leu (P2), 116.

All of the labeled samples were mixed with equal amounts, and then fractionated using a high-performance liquid chromatography (HPLC) system (Durashell C18 5 be 100 Å; 250 mm × 4.6 mm) (Thermo DINOEX Ultimate 3000 BioRS). A total of 20 fractions were collected in the end. LC-MS/MS analysis was performed as previously described [51]. For protein identification, the original MS/MS file data were searched against the *Homo sapiens* Uniprot database with the corresponding parameters for iTRAQ. Only proteins with at least one unique peptide and unused value more than 1.3 were considered for further analysis. Proteins with unique peptide > 1, fold change > 1.20 or < 0.83 and *P*-value < 0.05 were considered as differentially abundant. The MS proteomics data have been deposited to the ProteomeXchange Consortium via the PRIDE partner repository [52] with the data set identifier PXD007811. Gene Ontology (GO) analysis was performed using Blast2GO program.

Nuclear and cytoplasmic fractionation

Cells with 80% confluence were treated as indicated, and the nuclear and cytoplasmic fractionation was performed with a commercial nuclear and cytoplasmic extraction kit (ThermoFisher Scientific, 78,835) following the manufacturer's protocols.

Protein extraction and immunoblotting assays

Equal amounts of prepared protein samples were separated in sodium dodecyl sulfonate (SDS)-polyacrylamide gels, transferred onto polyvinylidene fluoride (PDVF) membranes, and blocked with 5% fat-free milk or bovine serum albumin (BSA [Roche, 738,328], for phosphorylation test of proteins) at room temperature for 1 h. Membranes were incubated at 4°C overnight with primary antibodies against indicated (phosphorylated) proteins. After incubation, the membranes were incubated with HRP-linked anti-rabbit or anti-mouse secondary antibody for 1 h at room temperature, developed with enhanced chemiluminescence method, and visualized by Kodak films. The images were quantified using ImageJ software.

DNA constructs, mutagenesis, and transfection

The pRK5-*HA-RPTOR* (8513; deposited by David Sabatini group) and pRK5-*FLAG-SZT2* (87,034; deposited by David Sabatini group) recombinant plasmids were obtained from Addgene. The plasmids PX459M and EZ-Guide were provided by Huabin He. To generate *CANX-MYC* fusion plasmid, cDNA encoding human *CANX* was cloned into pcDNA4/TO/MYC-His B plasmid. The pRK5-*CANX-FLAG* fusion plasmid was generated by inserting the *CANX*-encoding cDNA into the sites *Eco*R I and *Not* I of the pRK5-*FLAG-SZT2* plasmid, the primers used for amplification were: forward, TCGGTTCTATCGATTGAATTCATGGAAGGGAAGTGG-TTGCTGT; reverse: ATCCTTACTTACTTAGCGGCCGCTCACTTGTCATCGT-CATCCTTGTAGTCACCACCACCACCCTCTCTTCGTGG-CTTTCTGTTTC. The *EGFP-TMEM192* plasmid was generated by inserting human *TMEM192*-encoding cDNA into the sites *Hind* III and *Bam*H I of the *EGFP-MAP1LC3B* plasmid. All mutant plasmids (pRK5-*CANX-FLAG* K89R, K525R, and K89R+K525R were constructed based on the pRK5-*CANX-FLAG* plasmid, and pRK5-*MYC-RRAG GTPases* mutants) were generated using a commercial Fast MultiSite Mutagenesis System (TransGen Biotech, FM201). For transfection assays, cells with 80% confluence were transfected with indicated plasmids using the Lipo6000 (C0526) or Lipo8000 (C0533) transfection reagents (Beyotime Biotechnology). Six h later, cells were passed and cultured for another 36 h before treatments.

Immunofluorescence and confocal microscopy

Cells or transfected cells were planted in plates with poly-D-lysine-coated coverslips, cultured for 18 h and treated as indicated. After the treatments, cells grown on coverslips were rinsed with PBS once, and fixed with 4% paraformaldehyde solution at room temperature for 20 min. After washed with PBS for three times, cells were permeabilized with 0.2% Triton X-100 (in PBS) at room temperature for 20 min. Coverslips were washed three times with PBS, then cells were blocked with 5% BSA (in PBS) for 2 h at room temperature followed by incubation with primary antibodies (in BSA solution) (LAMP2, 1:300; MTOR, 1:400; MAP1LC3B, ProteinTech, 1:1000; CANX, 1:400) for 2 h at room temperature. Cells were rinsed with PBS 4 times, and incubated with secondary antibodies (diluted 1:1000 in BSA solution) for 1 h at room temperature in the dark. The coverslips were then rinsed with PBS 5 times, took out, fixed onto slides with mounting media, and observed with laser scanning confocal microscope (Zeiss LSM 800 META UV/Vis). Quantifications were performed using ImageJ software (version 1.51s) coupled with Colocalization_Finder plugin.

Generation of gene knockout cell lines

To generate *RRAGA, RRAGB, KAT7*, and *LAMP1* knockout cell lines, oligonucleotides encoding the guide RNAs (sgRNA) targeting the indicated gene loci were cloned into a modified PX459 (PX459M) vector containing coupled Cas9. To generate *CANX* and *LAMP2* knockout cell lines, two pairs of sgRNAs were cloned into the PX459M vector. The oligonucleotides used were:

sg*GFP*: Sense, caccgAGCACTGCACGCCGTAGGTC, Antisense, aaacGACCTACGGCGTGCAGTGCTc;
sg*CANX*: Sense 1, caccGGGCCCGTTGCAGCGAACGC, Antisense 1, aaacGCGTTCGCTGCAACGGGCCC; Sense 2, caccgTACTACTAGGGGTACCTAGT, Antisense 2, aaacACTAGGTACCCCTAGTAGTAc;
sg*RRAGA*: Sense, caccGGAGTGTTCCACGTCAATGG, Antisense, aaacCCATTGACGTGGAACACTCC;
sg*RRAGB*: Sense, caccGCCAGAGACACACGTCGCCT, Antisense, aaacAGGCGACGTGTGTCTCTGGC;
sg*LAMP1*: Sense, caccgCCGGCCGCCTCGCGCCATGG, Antisense, aaacCCATGGCGCGAGGCGGCCGGc.
sg*LAMP2*: Sense 1, caccgAGCTGTGCGGTCTTATGCAT, Antisense 1, aaacATGCATAAGACCGCACAGCTc; Sense 2, caccgCTTGGTAAAATTCGCAATCC, Antisense 2, aaacGGATTGCGAATTTTACCAAGc;
sg*KAT7*: Sense, caccgAGCCGCCGGCAATGCCGCGA, Antisense, aaacTCGCGGCATTGCCGGCGGCTc.

Then the constructs were transfected or co-transfected into HEK293T cells. Thirty-six h later, the cells were passed and cultured in fresh media containing 2 μg/mL puromycin for selection of 2 weeks. After selection, the mono-clones were cultured, and verified for on-targets by genomic DNA sequencing following genomic PCR. The genomic PCR primers used were: *CANX*-forward, ctgtatctctctgccctgacac, *CANX*-reverse, ctataatcccagcaccatcagtac; *RRAGA*-forward, gcgtatctccc-gagccgttgc, *RRAGA*-reverse, ctcaggtcttcctctcgctcttta; *RRAGB*-forward, tgtaattctgtcacctaaaggatgt, *RRAGB*-reverse, caaaaagttggacaagggcaat; *LAMP1*-forward, tggtaacgccgctgtctc-taa, *LAMP1*-reverse, ctgagaccacagacgtccct; *LAMP2*-forward, atgtcaccagtctgagccatga, *LAMP2*-reverse, atggggtcagtgggagggt-tat; *KAT7*-forward, gttccaccactggagtcactttct, *KAT7*-reverse, attcgggccacccaatcgag.

After confirmed the knockout of indicated proteins, cells were treated, and lysed for subsequent immunoblotting assays, or treated for confocal assays.

Immunoprecipitation, and mass spectrometric analysis

Cells were treated as indicated, lysed for 30 min at 4°C in IP lysis buffer (1% Triton X-100, 40 mM HEPES, pH 7.4, 10 mM β-glycerol phosphate [Sigma, G5422], 10 mM pyrophosphate [Sigma, S6422], 2.5 mM $MgCl_2$, supplemented with EDTA-free protease inhibitor cocktails, PhosStop [Sigma, 04906845001], and deacetylase inhibitor cocktails [Beyotime Biotechnology, P1113]), and centrifuged for 10 min at 14,000 x g at 4°C. The supernatants were added to 50% slurry of FLAG-M2 beads that were pre-washed with IP lysis buffer 3 times. After 2 h incubation with gentle rotation at 4°C, the beads were centrifuged and washed with IP lysis buffer containing 500 mM NaCl 4 times. Immunoprecipitates were denatured by adding 1× protein loading buffer followed by boiling for 6 min at 95°C before immunoblotting tests. For the IP assays in Figure 8, before cell lysis, cells were washed with PBS and incubated with 2 mM DSP crosslinker

(ThermoFisher Scientific, 22,585) for 15 min at room temperature, and washed with PBS and 20 mM Tris. For in vitro IP assays, the purified HA-RPTOR, crude lysosome fraction (CLF(-)), and S100(-) were mixed with or without leucine and incubated at 37°C for 30 min. The reaction tubes were transferred on ice to terminate the reaction, and subsequently centrifuged (17,800 x g, 4°C, 15 min) to separate the lysosome-enriched fractions from soluble proteins. The pellets were lysed in IP lysis buffer and incubated with antibodies against RRAGA at 4°C overnight. After being washed 3 times, immunoprecipitates were denatured by adding 1× protein loading buffer followed by boiling for 6 min at 95°C before immunoblotting tests. For MS analysis, 3 × 175 cm^2 flasks of HEK293T cells for each group transfected with corresponding FLAG-tagged plasmids were treated as indicated, lysed for 30 min at 4°C in IP lysis buffer, and incubated with FLAG-M2 beads, the beads were centrifuged and washed with IP lysis buffer containing 500 mM NaCl 4 times. The beads were further subjected into low pH elute buffer (0.1 M glycine, pH 2.0) and rotated for 5 min at room temperature, and neutralized with neutralization buffer (1 M Tris, pH 8.0). The eluted immunoprecipitates were analyzed by LC-MS/MS. Briefly, the immunoprecipitates were precipitated with TCA, washed with acetone, and dried. The dried fractions were dissolved in buffer (8 M urea, 100 mM Tris, pH 8.0), incubated in 10 mM DTT, followed by incubation in IAA. The proteins were digested with trypsin, desalted with a Sep-Pak C18 column and vacuum-dried. The MS analysis was performed with TripleTOF 5600 + .

GTP-binding assays

Cells were treated, and lysed with lysis buffer containing 1% Triton X-100 dissolved in PBS supplemented with EDTA-free protease inhibitor cocktails. Cell lysates were centrifuged for 10 min at 14,000 x g at 4°C. The supernatants were added to 50% slurry of γ-amino-hexyl-GTP beads that were pre-washed with lysis buffer 3 times. After 2 h incubation with gentle rotation at 4°C, the beads were centrifuged and washed with lysis buffer 3 times and with PBS once. The beads were denatured by adding 1× protein loading buffer followed by boiling for 10 min at 70°C before immunoblotting tests.

Immunoprecipition-based lysosome fractionation

The immunoprecipition-based lysosome fractionation was performed as previously described with minor modifications [28,29]. Briefly, WT or *ATG5* KO HEK293T cells overexpressing Tmem192-3× HA was treated as indicated. Cells were harvested, 2.5% cells were kept to extract total proteins as whole cell lysate (WCL), while the other fractions were homogenized in ice-cold PBS supplemented with protease inhibitor cocktail, and cleared homogenates were incubated with anti-HA magnetic beads. After wash steps, lysosomal proteins were extracted by incubating the beads with lysis buffer.

In vitro crotonylation assay

Recombinant GST-KAT7, GST-CANX WT, and GST-CANX K525R were expressed in bacteria and purified. Briefly, pGEX4T-1-based plasmids were transformed into Rosetta bacteria, and monoclones were grown in LB supplemented with ampicillin at 37°C to an attenuance of nearly 0.6 at 600 nm followed by induction of 0.3 mM IPTG for 12 h at 28°C. The cells were washed with ice-cold PBS twice and resuspended in PBS supplemented with 0.2 mg/mL Lysozyme and 1 mM PMSF, followed by pressure broken and centrifugation. The clear lysates were incubated with Glutathine Sephagrose 4B (GE Healthcare) for 2 h at 4°C with gently rotation. The sepharoses were washed with PBS 5 times, and incubated with elute buffer (20 mM glutathione, 50 mM Tris-HCl, pH 8.0) for 2 h at 4°C. The resulting elutes were added with 20% glycerol and aliquots at −80°C before used. For *in vitro* crotonylation assay, 1 μg GST-CANX WT or GST-CANX K525R were incubated with 0.1 μg GST-KAT7 in reaction buffer (50 mM Tris pH 8.0, 10% glycerol, 150 mM NaCl and 1 mM DTT) at 37°C for 2 h with or without 100 μM crotonyl-CoA (Sigma, 28,007). The reactions were terminated by adding SDS sample buffer and heated to 95°C before analyzed by SDS-PAGE.

Statistical analysis

All quantification of immunoblots was done with ImageJ software, all quantification of colocalization in immunostaining assays was performed with Coloc2 plugin of ImageJ (Fiji) software. All statistical analysis was done using the GraphPad Prism software (version 6.0c, Graphpad Software Inc., La Jolla, CA, USA). Statistical significance was calculated by two-tailed Student's *t*-test. Differences were considered statistically significant at $P < 0.05$.

Abbreviations

CALR, calreticulin; CANX, calnexin; CLF, crude lysosome fraction; EIF4EBP1, eukaryotic translation initiation factor 4E binding protein 1; ER, endoplasmic reticulum; GST, glutathione S-transferase; HA, hemagglutinin; HEK293T, human embryonic kidney-293T; KAT7, lysine acetyltransferase 7; Kcr; lysine crotonylation; KO, knockout; LAMP2, lysosomal associated membrane protein 2; LAMTOR/Ragulator, late endosomal/lysosomal adaptor, MAPK and MTOR activator; MAP1LC3B, microtubule associated protein 1 light chain 3 beta; MTOR, mechanistic target of rapamycin kinase; PDI, protein disulfide isomerase; PTM, post-translational modification; RPS6KB1/p70S6 kinase 1, ribosomal protein S6 kinase B1; RPTOR, regulatory associated protein of MTOR complex 1; SESN2, sestrin 2; TMEM192, transmembrane protein 192; ULK1, unc-51 like autophagy activating kinase 1.

Acknowledgments

We thank all Yan laboratory members for critical discussion and reading of the manuscript. The plasmids PX459M and EZ-Guide were kindly provided by Huabin He (Tsinghua University, China). The *ATG5* knockout HEK293T cell line was a kind gift from Prof. Jun Cui (Sun Yat-sen University, China), the AML12 cell line was a kind gift from Prof. Rui Zhou (Wuhan University, China).

Disclosure statement

No potential conflict of interest was reported by the author(s).

Funding

This work was supported by the National Natural Science Foundation of China (31520103915), the National Key Basic Research Program of China (973 Program) (National Basic Research Program of China (973 Program) 2013CB127305), Hubei Provincial Natural Science Foundation of China (Natural Science Foundation of Hubei Province 2018CFA020), and the Fundamental Research Funds for the Central Universities (2013PY056, 2662015PY111, and 2013JQ001).

References

[1] Eltschinger S, Loewith R. TOR complexes and the maintenance of cellular homeostasis. Trends Cell Biol. 2016;26:148–159. PMID:26546292.
[2] Zoncu R, Efeyan A, Sabatini DM. mTOR: from growth signal integration to cancer, diabetes and ageing. Nat Rev Mol Cell Biol. 2011;12:21–35. PMID:21157483.
[3] Jewell JL, Russell RC, Guan KL. Amino acid signalling upstream of mTOR. Nat Rev Mol Cell Biol. 2013;14:133–139. PMID:23361334.
[4] Chauvin C, Koka V, Nouschi A, et al. Ribosomal protein S6 kinase activity controls the ribosome biogenesis transcriptional program. Oncogene. 2014;33:474–483. PMID:23318442.
[5] Dibble CC, Manning BD. Signal integration by mTORC1 coordinates nutrient input with biosynthetic output. Nat Cell Biol. 2013;15:555–564. PMID:23728461.
[6] Saxton RA, Sabatini DM. mTOR signaling in growth, metabolism, and disease. Cell. 2017;168:960–976. PMID:28283069.
[7] Ma XM, Blenis J. Molecular mechanisms of mTOR-mediated translational control. Nat Rev Mol Cell Biol. 2009;10:307–318. PMID:19339977.
[8] Holz MK, Ballif BA, Gygi SP, et al. mTOR and S6K1 mediate assembly of the translation preinitiation complex through dynamic protein interchange and ordered phosphorylation events. Cell. 2005;123:569–580. PMID:16286006.
[9] Sancak Y, Bar-Peled L, Zoncu R, et al. Ragulator-rag complex targets mTORC1 to the lysosomal surface and is necessary for its activation by amino acids. Cell. 2010;141:290–303. PMID:20381137.
[10] Sancak Y, Peterson TR, Shaul YD, et al. The rag gTPases bind raptor and mediate amino acid signaling to mTORC1. Science. 2008;320:1496–1501. PMID:18497260.
[11] Bar-Peled L, Schweitzer LD, Zoncu R, et al. Ragulator is a GEF for the rag gTPases that signal amino acid levels to mTORC1. Cell. 2012;150:1196–1208. PMID:22980980.
[12] Chiang GG, Abraham RT. Phosphorylation of mammalian target of rapamycin (mTOR) at ser-2448 is mediated by p70S6 kinase. J Biol Chem. 2005;280:25485–25490. PMID:15899889.
[13] Soliman GA, Acosta-Jaquez HA, Dunlop EA, et al. mTOR ser-2481 autophosphorylation monitors mTORC-specific catalytic activity and clarifies rapamycin mechanism of action. J Biol Chem. 2010;285:7866–7879. PMID:20022946.
[14] Ekim B, Magnuson B, Acosta-Jaquez HA, et al. mTOR kinase domain phosphorylation promotes mTORC1 signaling, cell growth, and cell cycle progression. Mol Cell Biol. 2011;31:2787–2801. PMID:21576368.
[15] Gwinn DM, Shackelford DB, Egan DF, et al. AMPK phosphorylation of raptor mediates a metabolic checkpoint. Mol Cell. 2008;30:214–226. PMID:18439900.
[16] Ber Y, Shiloh R, Gilad Y, et al. DAPK2 is a novel regulator of mTORC1 activity and autophagy. Cell Death Differ. 2015;22:465–475. PMID:25361081.
[17] Dunlop EA, Hunt DK, Acosta-Jaquez HA, et al. ULK1 inhibits mTORC1 signaling, promotes multisite raptor phosphorylation and hinders substrate binding. Autophagy. 2011;7:737–747. PMID:21460630.
[18] Son SM, Park SJ, Lee H, et al. Leucine signals to mtorc1 via its metabolite acetyl-coenzyme A. Cell Metab. 2019;29:192–201.e197. PMID:30197302.
[19] Garcia-Aguilar A, Guillen C, Nellist M, et al. TSC2 N-terminal lysine acetylation status affects to its stability modulating mTORC1 signaling and autophagy. Biochim Biophys Acta. 2016;1863:2658–2667. PMID:27542907.
[20] Sabari BR, Zhang D, Allis CD, et al. Metabolic regulation of gene expression through histone acylations. Nat Rev Mol Cell Biol. 2017;18:90–101. PMID:27924077.
[21] Harris DC, Jewett MC. Cell-free biology: exploiting the interface between synthetic biology and synthetic chemistry. Curr Opin Biotechnol. 2012;23:672–678. PMID:22483202.
[22] Liu AP, Fletcher DA. Biology under construction: in vitro reconstitution of cellular function. Nat Rev Mol Cell Biol. 2009;10:644–650. PMID:19672276.
[23] Hodgman CE, Jewett MC. Cell-free synthetic biology: thinking outside the cell. Metab Eng. 2012;14:261–269. PMID:21946161.
[24] Yan X, Sun Q, Ji J, et al. Reconstitution of leucine-mediated autophagy via the mTORC1-barkor pathway in vitro. Autophagy. 2012;8:213–221. PMID:22258093.
[25] Zoncu R, Bar-Peled L, Efeyan A, et al. mTORC1 senses lysosomal amino acids through an inside-out mechanism that requires the vacuolar H(+)-aTPase. Science. 2011;334:678–683. PMID:22053050.
[26] Ren Y, Hao P, Law SK, et al. Hypoxia-induced changes to integrin alpha 3 glycosylation facilitate invasion in epidermoid carcinoma cell line A431. Mol Cell Proteomics. 2014;13:3126–3137. PMID:25078904.
[27] Garofalo T, Matarrese P, Manganelli V, et al. Evidence for the involvement of lipid rafts localized at the ER-mitochondria associated membranes in autophagosome formation. Autophagy. 2016;12:917–935. PMID:27123544.
[28] Wyant GA, Abu-Remaileh M, Frenkel EM, et al. NUFIP1 is a ribosome receptor for starvation-induced ribophagy. Science. 2018;360:751–758. PMID:29700228.
[29] Abu-Remaileh M, Wyant GA, Kim C, et al. Lysosomal metabolomics reveals V-aTPase- and mTOR-dependent regulation of amino acid efflux from lysosomes. Science. 2017;358:807–813. PMID:29074583.
[30] Klionsky DJ, Abdelmohsen K, Abe A, et al. Guidelines for the use and interpretation of assays for monitoring autophagy (3rd edition). Autophagy. 2016;12:1–222. PMID:26799652.
[31] Sabari BR, Tang Z, Huang H, et al. Intracellular crotonyl-coA stimulates transcription through p300-catalyzed histone crotonylation. Mol Cell. 2015;58:203–215. PMID:25818647.
[32] Xu W, Wan J, Zhan J, et al. Global profiling of crotonylation on non-histone proteins. Cell Res. 2017;27:946–949. PMID:28429772.
[33] Liu X, Wei W, Liu Y, et al. MOF as an evolutionarily conserved histone crotonyltransferase and transcriptional activation by histone acetyltransferase-deficient and crotonyltransferase-competent CBP/p300. Cell Discov. 2017;3:17016. PMID:28580166.
[34] Han JM, Jeong SJ, Park MC, et al. Leucyl-tRNA synthetase is an intracellular leucine sensor for the mTORC1-signaling pathway. Cell. 2012;149:410–424. PMID:22424946.
[35] Saxton RA, Knockenhauer KE, Wolfson RL, et al. Structural basis for leucine sensing by the sestrin2-mTORC1 pathway. Science. 2016;351:53–58. PMID:26586190.
[36] Shibata Y, Shemesh T, Prinz WA, et al. Mechanisms determining the morphology of the peripheral ER. Cell. 2010;143:774–788. PMID:21111237.
[37] Drenan RM, Liu X, Bertram PG, et al. FKBP12-rapamycin-associated protein or mammalian target of rapamycin (FRAP/mTOR) localization in the endoplasmic reticulum and the golgi apparatus. J Biol Chem. 2004;279:772–778. PMID:14578359.

[38] Roderick HL, Lechleiter JD, Camacho P. Cytosolic phosphorylation of calnexin controls intracellular Ca(2+) oscillations via an interaction with SERCA2b. J Cell Biol. 2000;149:1235–1248. PMID:10851021.
[39] Guo Y, Li D, Zhang S, et al. Visualizing intracellular organelle and cytoskeletal interactions at nanoscale resolution on millisecond timescales. Cell. 2018;175:1430–1442.e1417. PMID:30454650.
[40] Lim CY, Davis OB, Shin HR, et al. ER-lysosome contacts enable cholesterol sensing by mTORC1 and drive aberrant growth signalling in niemann-pick type C. Nat Cell Biol. 2019;21:1206–1218. PMID:31548609.
[41] Li M, Zhang CS, Zong Y, et al. Transient receptor potential v channels are essential for glucose sensing by aldolase and AMPK. Cell Metab. 2019;30:508–524.e512. PMID:31204282.
[42] Tan M, Luo H, Lee S, et al. Identification of 67 histone marks and histone lysine crotonylation as a new type of histone modification. Cell. 2011;146:1016–1028. PMID:21925322.
[43] Liu S, Yu H, Liu Y, et al. Chromodomain protein cdyl acts as a crotonyl-coa hydratase to regulate histone crotonylation and spermatogenesis. Mol Cell. 2017;67:853–866.e855. PMID:28803779.
[44] Wu Q, Li W, Wang C, et al. Ultradeep lysine crotonylome reveals the crotonylation enhancement on both histones and nonhistone proteins by saha treatment. J Proteome Res. 2017;16:3664–3671. PMID:28882038.
[45] Li X, Yu W, Qian X, et al. Nucleus-translocated acss2 promotes gene transcription for lysosomal biogenesis and autophagy. Mol Cell. 2017;66:684–697.e689. PMID:28552616.
[46] Li X, Jiang Y, Meisenhelder J, et al. Mitochondria-translocated pgk1 functions as a protein kinase to coordinate glycolysis and the tca cycle in tumorigenesis. Mol Cell. 2016;61:705–719. PMID:26942675.
[47] Lee JH, Liu R, Li J, et al. EGFR-phosphorylated platelet isoform of phosphofructokinase 1 promotes pi3k activation. Mol Cell. 2018;70:197–210.e197. PMID:29677490.
[48] Yan G, Li X, Peng Y, et al. The fatty acid beta-oxidation pathway is activated by leucine deprivation in hepg2 cells: a comparative proteomics study. Sci Rep. 2017;7:1914. PMID:28507299.
[49] Zou C, Chen Y, Smith RM, et al. SCF(Fbxw15) mediates histone acetyltransferase binding to origin recognition complex (HBO1) ubiquitin-proteasomal degradation to regulate cell proliferation. J Biol Chem. 2013;288:6306–6316. PMID:23319590.
[50] Wu JC, Merlino G, Fausto N. Establishment and characterization of differentiated, nontransformed hepatocyte cell lines derived from mice transgenic for transforming growth factor alpha. Proc Natl Acad Sci U S A. 1994;91:674–678. PMID:7904757.
[51] Yan G, Li X, Cheng X, et al. Proteomic profiling reveals oxidative phosphorylation pathway is suppressed in longissimus dorsi muscle of weaned piglets fed low-protein diet supplemented with limiting amino acids. Int J Biochem Cell Biol. 2016;79:288–297. PMID:27590855.
[52] Vizcaino JA, Csordas A, Del-toro N, et al. 2016 update of the PRIDE database and its related tools. Nucleic Acids Res. 2016;44:D447–456. PMID:26527722.